Examining the Feasibility of a Novel Ground-Storage Cooling System

by

Nicole Tang Liwen

Bachelor of Science in Mechanical Engineering (BSME), Tufts University (2015)

Submitted to the Department of Architecture
in partial fulfillment of the requirements for the degree of

Master of Science in Building Technology

at the

MASSACHUSETTS INSTITUTE OF TECHNOLOGY

September 2020

Author .....
Department of Architecture
August 7, 2020

Certified by .....
Leon R. Glicksman
Professor of Building Technology
Thesis Supervisor

Accepted by .....
Leslie K. Norford
Professor of Building Technology
Chairman, Department Committee on Graduate Students

Examining the Feasibility of a Novel Ground-Storage Cooling System

by

Nicole Tang Liwen

Submitted to the Department of Architecture
on August 7, 2020, in partial fulfillment of the
requirements for the degree of
Master of Science in Building Technology

Abstract

The Boston climate is known for its long, cold winters but it also suffers from hot, humid summers. The dehumidification needed to maintain occupant comfort in summer is often provided by condensing the excess moisture onto surfaces cooled by cold water. The systems currently used to provide the cold water have limited efficiencies, so alternative systems must be sought in order to achieve reductions in building energy use and to reduce the rate of climate change.

This research examines the feasibility of a ground-cooling storage system that stores the abundant Boston winter cold in an underground block of soil to provide dehumidification in summer. In winter, heat exchangers use the cold air to produce cold water, which flows through a set of pipes in the soil block, cooling the soil. In summer, the cooling stored in the soil block is used to provide cold water for the dehumidifier, thus meeting the latent cooling loads of the building.

The physical scale of the system required was found to be reasonable, relative to typical building sizes. The soil block, which does not use any valuable program space, was sized as less than 10% of the overall building size and did not require deep excavation. Winter thermal modeling showed that the soil block could be fully charged in a typical winter season. The summer thermal modeling showed that the system can meet the majority of the building cooling loads and is capable of responding to cooling peaks.

The system energy use is primarily driven by the use of the heat exchangers for winter charging. The system was estimated to have a coefficient of performance of 71, which is much higher than that of comparable systems used for dehumidification. In conclusion, this feasibility study found that the proposed system shows promising results as an alternative to conventional systems and is worth further investigation.

Thesis Supervisor: Leon R. Glicksman
Title: Professor of Building Technology

Acknowledgments

As connected as we are in this digital age, it is admittedly quite odd to finish this degree in a time of social distancing and isolation. Although we cannot all be physically present in the same room, I would like to express my deepest gratitude to all who have helped me in completing this degree.

First, I would like to thank my advisor, Professor Leon Glicksman, for his insight, guidance, and patience. Many of our meetings that began with my reluctant admission that research hadn't been going as smoothly as hoped and that I wasn't sure what to do next. These meetings always ended with a plan for the following week and the reassurance that I wasn't the least capable graduate researcher to have ever walked through Lobby 7. I am grateful to have had the opportunity to work with you and to learn from you. Professor Les Norford, thank you for bringing me into the VolpeMIT project and providing valuable feedback along the development of this thesis. It was truly a learning experience to be your teaching assistant during the transition to distance learning.

To the Building Technology faculty, staff, and fellow students, thank you for fostering a supportive and caring environment. Whether it was commiserating over failures or celebrating successes or just having a good chat, I'm glad to have spent the last two years with such lovely people.

To all of my friends, old and new, thank you for reminding me that there is a world beyond this degree. You have helped me in so many ways and my life is richer for having you in it.

Finally, I'd like to thank my family for their endless love and support. Mark and Sam, thank you for always welcoming me into your home and taking care of me. Mum and Dad, I am here because of all the opportunities and advantages that you have worked to give to me and so there is a lot of gratitude to fit into very few words, but thank you for everything.

Contents

List of Figures

List of Tables

Acronyms

COP Coefficient of Performance.

DOAS Dedicated Outdoor Air System.

EWT Entering Water Temperature.

GCM Graphical Comfort Zone Method.

HX Heat Exchanger.

LWT Leaving Water Temperature.

OAHR Outside Air Humidity Ratio.

PDE Partial Differential Equation.

PMV Predicted Mean Vote.

SAHR Supply Air Humidity Ratio.

Chapter 1

Introduction

1.1 Objective

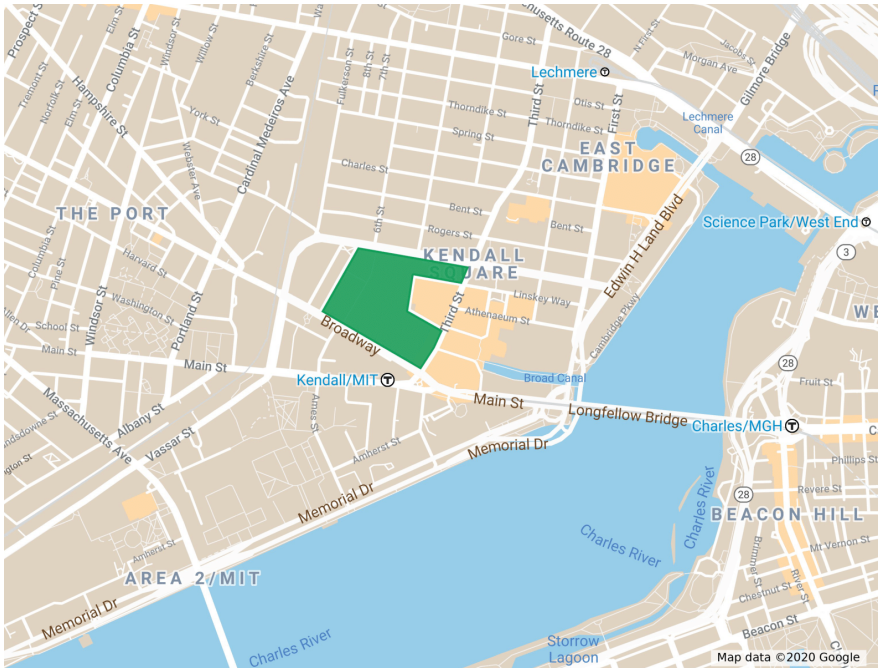

Figure 1-1: Map of Cambridge area with VolpeMIT plot highlighted in green (Google, nd)

This research was conducted as part of a research program to identify opportunities for energy efficient designs for the new buildings of the VolpeMIT development project. The project is a mixed-use development, including residential, commercial, and public use open

space, near the Kendall Square area in Cambridge, Massachusetts (Cambridge, 2017). This area experiences both harsh winters and hot and humid summers. Data from the current Boston EnergyPlus weather file (National Renewable Energy Laboratory, nd), plotted in Figure 1-2, shows that the temperature and humidity values cover a large range. A novel ground-storage cooling system is proposed to take advantage of this range to store the abundance of winter 'coolth' to serve the cooling needs in the summer.

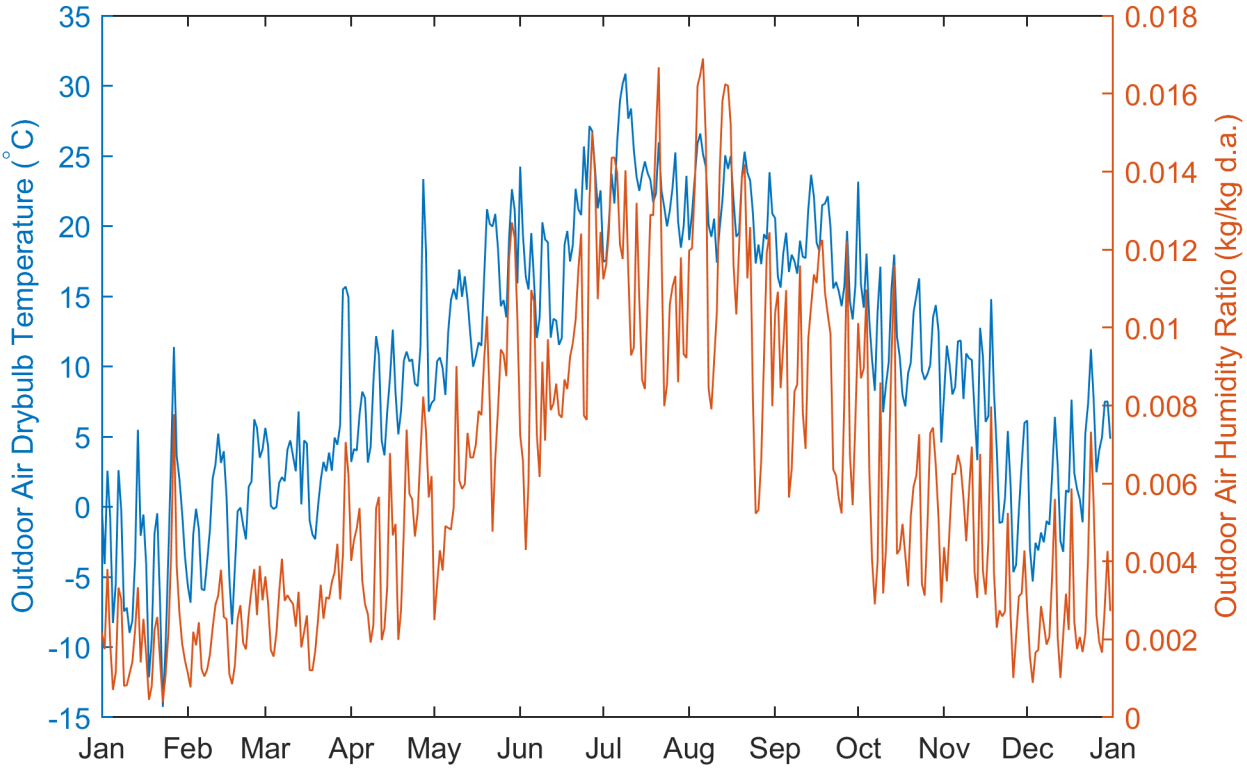

Figure 1-2: Daily average outdoor air drybulb temperatures and humidity ratios

This thesis aims to examine the feasibility of using the proposed system to provide latent cooling to a building in the VolpeMIT development. Of the building types anticipated on the site, an office building was chosen as the building type served by the proposed system. As the building designs have not yet been determined, a generic office building was assumed based on typical office inputs.

1.2 Context

Measured data has shown that the Earth is warming and that the likely cause for this is the anthropogenic emission of greenhouse gases. The average temperature over land in 2006-2015 was 1.5K higher than in 1850-1900 (IPCC, 2014). The effect of this warming is far-reaching, causing rising sea-levels, desertification of arable land, and a loss of habitat for animals and humans alike. In a business-as-usual forecast scenario, the surface air temperature over the continental United States was found likely to rise 2.6 to 4.4K above pre-industrial temperatures by the end of the 21st century (Sokolov et al., 2017). As human activity is the driving factor behind this climate change, there is a responsibility to bring about anthropogenic mitigation of these emissions.

1.2.1 Building Cooling Energy

In 2019, commercial and residential buildings used 29% of the overall energy consumption in the US (EIA, 2020). Approximately 9% of all commercial building energy used in the US in 2012 was for cooling (EIA, 2016) and 8% of all residential building energy used in the US in 2015 was for cooling (EIA, 2018). As temperatures rise, these percentages are expected to grow significantly. Systems will not only operate for longer periods but will also have to cool from higher temperatures. Furthermore, the demand for cooling will increase in areas with climates that were previously considered mild or cool, such that the overall percentage of buildings needing cooling increases. Therefore, improving the efficiency of cooling systems not only reduces energy use in buildings, but also lessens the effect of increased demand in future climates.

The cooling load of buildings is split into two components: sensible and latent cooling. Sensible cooling refers to the lowering of the air temperature while latent cooling refers to the removal of moisture from the air. If only sensible cooling were provided, the room would feel excessively humid and the water in the air might condense onto cold surfaces. If only latent cooling were provided, the room would feel too warm. Although both types of cooling are typically needed simultaneously, it is most efficient to split the cooling load to handle them separately. This is because sensible loads can be handled with relatively warm water that

can be produced by high-efficiency systems such as ground-source heat pumps. In contrast, latent loads typically use cold water to condense the water vapor from the air. Producing this cold water generally requires the use of chiller systems, which are less efficient due to the limits of the vapor-compression cycle they use.

Although the cold water produced by the proposed system could be used for either type of cooling load, this thesis is primarily focused on meeting the latent load. The system would likely be prohibitively large if sized to meet the total cooling load and there are already existing efficient means of producing the water needed for sensible cooling. Therefore, using the proposed system to handle latent cooling loads only allows it to replace the least efficient aspect of building cooling.

1.3 Proposed Ground-Storage Cooling System

The proposed system consists of a soil block beneath the building, a cooling source that feeds the soil block, and a dehumidifier in the building. In winter mode, shown in Figure 1-3, the cooling source charges the soil block with cooling energy from the cold weather. In summer mode, shown in Figure 1-4, the soil block supplies the stored cooling energy to the dehumidifier to provide latent cooling to the building.

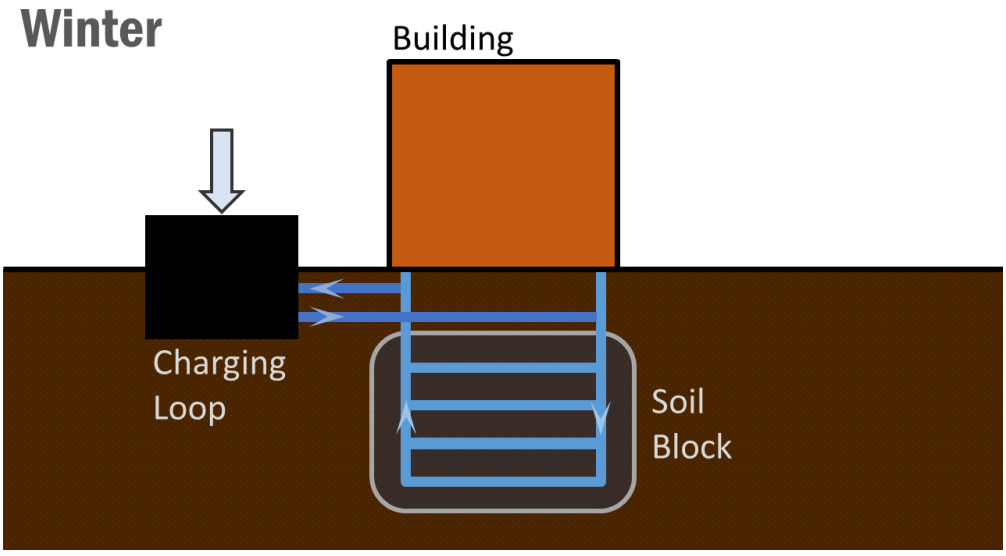

Figure 1-3: Diagram of proposed cooling system operating in winter

1.3.1 Soil Block

The soil block is analogous to a battery, storing cooling energy in winter to use in summer. The pipes that run through the soil block connect it to other components in the system by transferring cooling to and from the soil. The block is kept underground because deep soil temperatures are relatively constant throughout the year. This ensures that the surrounding soil will not have large temperature fluctuations that affect the soil block temperature. An insulating barrier could be placed around the soil block to ensure that heat and moisture within the enclosed block is not exchanged with the surrounding soil.

The proposed system places the soil block under the building to simplify the excavation process. When constructing the building, the construction team would excavate deeper than required for the foundation to install the pipes and backfill with the removed soil. Although soil has a lower specific heat capacity than water, reusing the excavated soil is economical (Bott et al., 2019). Furthermore, as the foundation is built on top of the soil block, using soil instead of water is also structurally advantageous.

1.3.2 Cooling Source

To use the winter weather to charge the soil block, the soil block must be connected to the cold outdoor air. Two possible components for providing this connection have been considered. These two options are discussed in greater depth in Chapter 5.

The first option is using a Heat Exchanger (HX) that is exposed to the cold outside air. This option is commercially available and does not require complex installation work. However, this requires fans to move the outside air through the HX, which could add a large amount of fan energy to the system, thereby reducing its overall efficiency.

The second option is a near-surface source loop. This is an additional soil block placed at a shallow depth in a location that is not covered by buildings. The pipes in this source block would be much closer to the outside air, allowing them to cool the water that they then send to the storage soil block. The entire system would only require pumping energy for moving the water through the pipes. Pumping energy is typically lower than fan energy, so the near-surface source loop is expected to use less energy than the heat exchanger option.

However, the excavation and installation costs of this option could be high, depending on the size of the component.

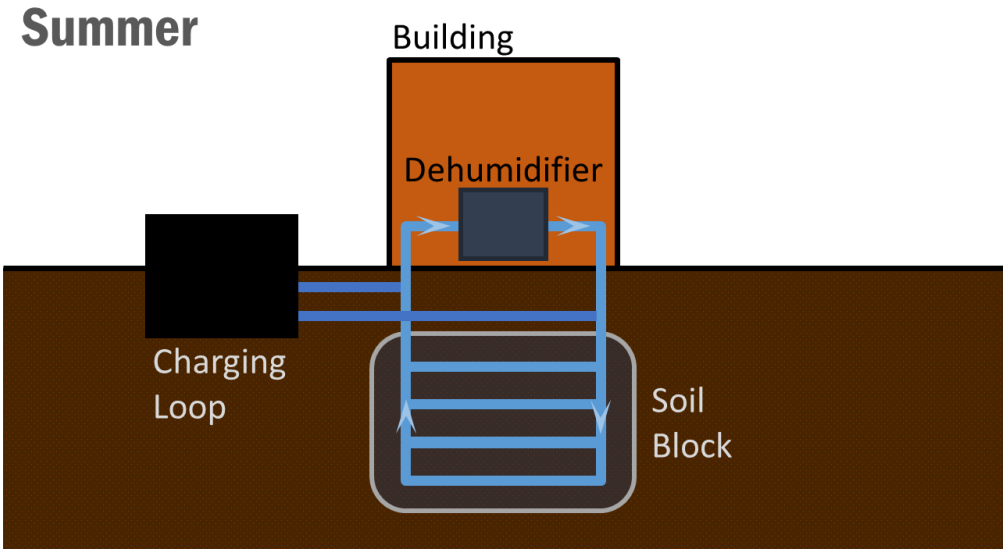

Figure 1-4: Diagram of proposed cooling system operating in summer

1.3.3 Dehumidifier

The dehumidifier is a heat exchanger in a Dedicated Outdoor Air System (DOAS), which removes moisture from the minimum amount of outdoor air needed for ventilation. Cold water is passed through the DOAS HX, which is kept below or at the dewpoint temperature associated with the desired humidity ratio. As the ventilation air passes over the HX, the excess water vapor in the air condenses on the cold HX surface until the air is sufficiently dry to be supplied to the rooms.

The cold water passing through the HX absorbs waste heat from the air in this process. It is then sent through the soil block to reject this waste heat into the cold soil. Once it has cooled to an acceptable temperature, it returns to the DOAS to repeat the cycle.

1.4 Comparable Systems

Of course, there are other cooling systems currently in use and in development that are worth understanding as comparisons against the proposed ground-storage cooling system.

The wide range of system types suggests that there is still room for alternative systems and strategies to be considered to improve the cooling of buildings.

1.4.1 Vapor-Compression

As previously mentioned, cold water for cooling is typically produced with chillers that run a vapor-compression cycle. This cycle uses the compression and expansion of a refrigerant to enable it to absorb heat from the warm incoming air. The performance of these chillers is capped by the Carnot limit on any thermodynamic cycle. This technology is well-established and manufacturers are working on moving chiller efficiencies towards the Carnot limit.

The use of refrigerants is a significant cause for concern as these materials have high global warming potentials (Goetzler et al., 2016). While refrigerant leakage may be minimal per chiller, the cumulative effect of many chillers is a significant source of anthropogenic emissions. Therefore, if the growth in cooling demand is simply met with the use of more chillers, the net impact of the refrigerant use may actually exacerbate the climate change that caused the demand increase, regardless of the chiller efficiencies.

1.4.2 Thermal Energy Storage

Thermal energy storage systems for air conditioning, similar to the proposed system, have existed since the mid-20th century (Lindsay and Andrepont, 2019). These systems use cheaper electricity during off-peak demand hours to charge the storage material, typically by freezing water into ice, although other fluids have also been used. This charged material is then used to provide cooling during the daytime, thus avoiding the use of the more expensive peak-demand electricity.

The proposed system would be considered a form of seasonal thermal energy storage as it is charged in winter to be discharged in summer. A similar system has been proposed by Yang et al. (2013) to utilize the cold winter weather in Harbin, China, to provide total cooling in summer for a $97\,\mathrm{m}^2$ test office space. The system they designed uses vertical borehole ground heat exchangers that are approximately 50 m deep to store the cooling. The results showed that their system was successful, which bodes well for the feasibility of this proposed

system. However, it was found that the temperature differences of the borehole between the charging and discharging operation modes diminished with borehole depth, suggesting that only a shallow section of the borehole was active in providing cooling. The system proposed in this thesis uses a relatively shallow soil block, with pipes running horizontally. If this orientation is shown to be successful, it would likely be more economical than the vertical borehole option, due to the reduced excavation depth.

1.4.3 Desiccant Dehumidification

These systems pass the humid air over a desiccant material that draws the water vapor out from the air, thus providing dehumidification (Chen, 2019). The absorbed water vapor must then be removed from the desiccant material for it to continue to work. This regeneration uses heat, which can be obtained as waste heat from a separate process or directly from an energy-using heat source. Since the desiccant material is warm, the incoming air picks up some sensible heat, thereby increasing the sensible cooling needed to bring the air to a comfortable temperature.

1.4.4 Membrane Dehumidification

Similar to the desiccant system, humid air is passed through a membrane stack that separates the water vapor from the air (Chen, 2019). In this case, a vacuum pump provides a vapor pressure differential across a hydrophilic semi-permeable membrane. Only the water vapor passes through the membrane, leaving the remaining air drier. The water vapor is then condensed into liquid water and pumped out of the system.

Alternatively, instead of condensing the water vapor, the vapor pump could be connected to another membrane stack. In this case, the relatively dry exhaust air is passed over the second membrane. The water vapor pulled from the first membrane passes through the second membrane where it is pulled into the exhaust air stream and rejected outdoors.

The membrane and desiccant systems are not affected by the Carnot limit as they do not use thermodynamic cycles. However, the energy needed for the additional processes of desiccant regeneration or vacuum pumping may be large in some cases. Although these

systems are promising, they are not always the most efficient means of providing latent cooling, depending on the local climate conditions (Chen, 2019).

Chapter 2

Cooling Loads

Before the proposed system can be evaluated, the latent cooling loads to be met must first be calculated to size the system components. These loads are driven by the weather conditions, the internal loads of the space, and the thermal comfort conditions applied.

2.1 Thermal Comfort Requirements

ASHRAE Standard 55-2017 was used to determine the indoor conditions that the system would need to meet (ASHRAE, 2017b). The metabolic rate and garment insulation limits of the Graphical Comfort Zone Method (GCM) were deemed suitable for typical office work. The comfort zone for office occupants with clothing factors ranging from 0.5 to 1 clo is outlined in red in Figure 2-1. This method states that the maximum allowable humidity ratio of the room air shall not exceed 0.012 kg/kg for all temperatures within the comfort range. It is possible for occupants to remain comfortable for humidity ratios higher than this but Predicted Mean Vote (PMV) method calculations would be needed in order to prove their comfort. The GCM humidity ratio limit is used for simplicity and the use of the PMV method is discussed in section 2.4.

The dehumidification component of the proposed DOAS is only required to provide sufficiently dry ventilation air such that the moisture level of the mixed room air is not uncomfortable for occupants. This air may be warmer or cooler than the desired room air temperature. However, it is assumed that the building would have a separate sensible sys-

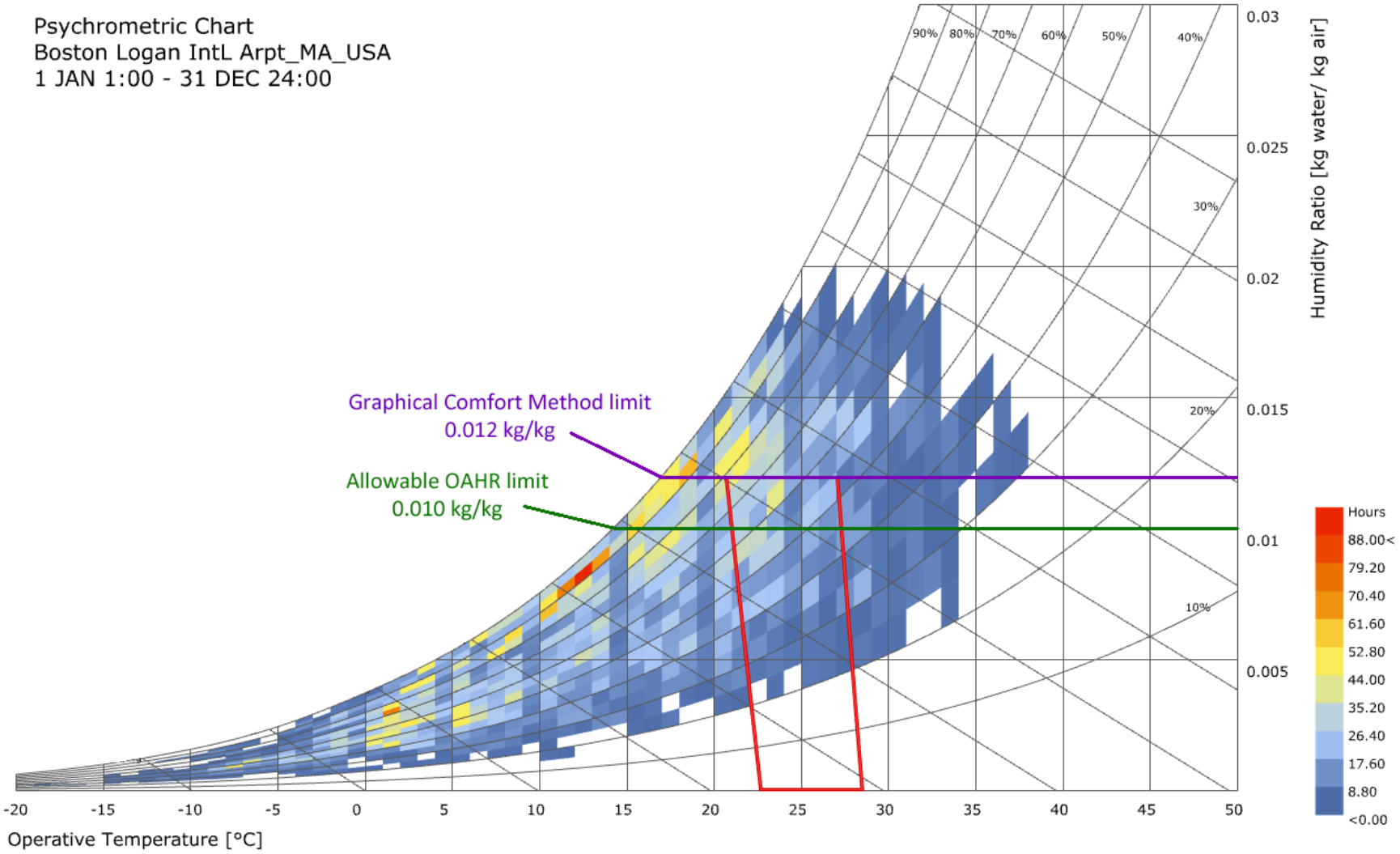

Figure 2-1: Psychrometric chart of Boston weather with humidity ratio comfort limits.
(Produced using Ladybug plugin for Grasshopper (Roudsari and Pak, 2013))

tem that can cool or warm the room locally to maintain thermal comfort. Therefore, the calculated latent loads are solely from the maintenance of the 0.012 kg/kg limit.

2.2 Latent Load Calculation Method

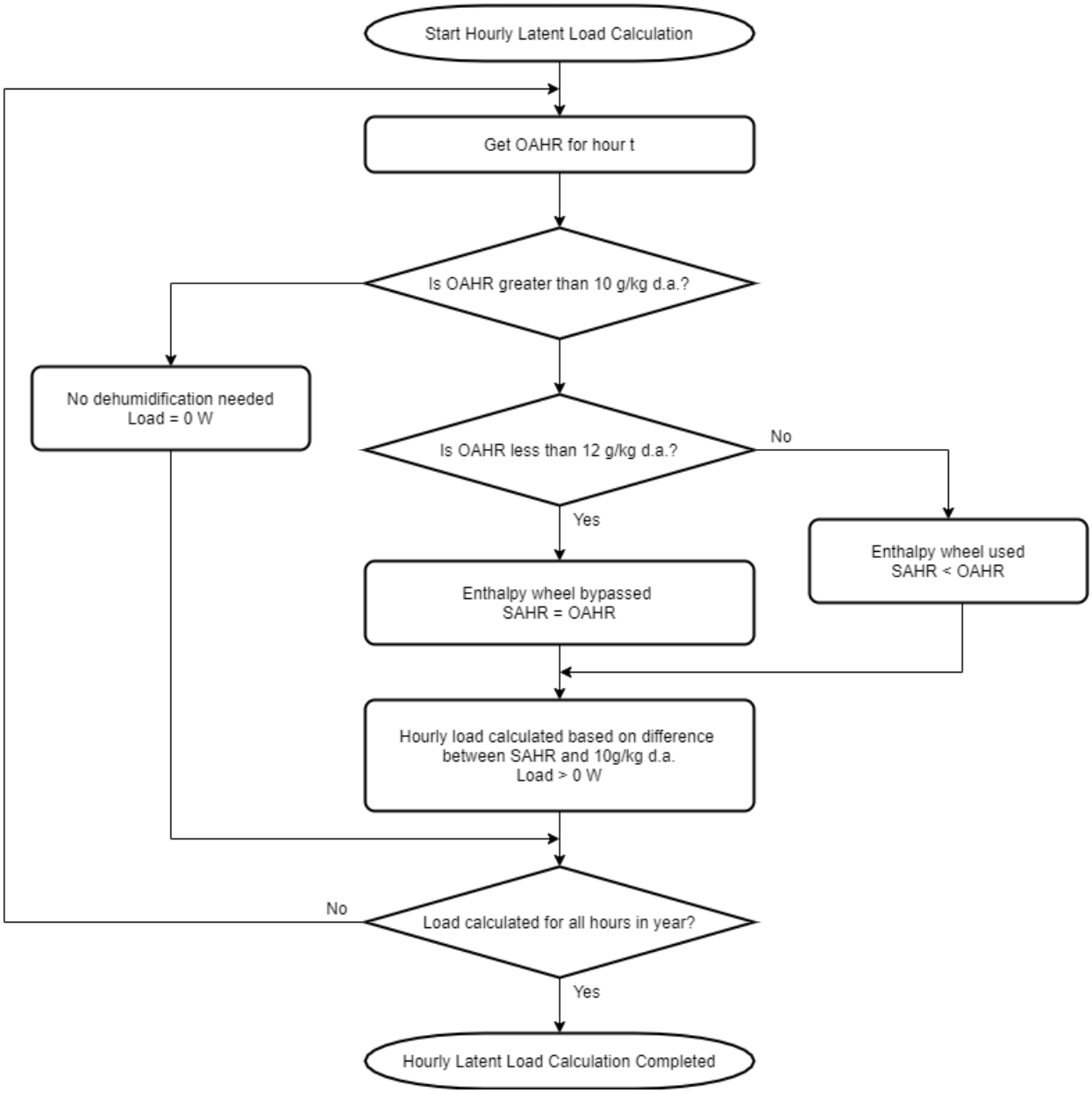

Figure 2-2: Flowchart for calculation of hourly latent loads based on weather data

The overall procedure for calculating the hourly latent cooling loads is outlined in Figure 2-2 and is described in detail in this section.

Table 2.1: Office Building Inputs for Latent Load Calculation

Building Geometry	
Floor Area	1760 m^2
Floor Height	4 m
Number of Floors	25
Building Equipment	
HVAC Equipment Schedule (ASHRAE, 2017c)	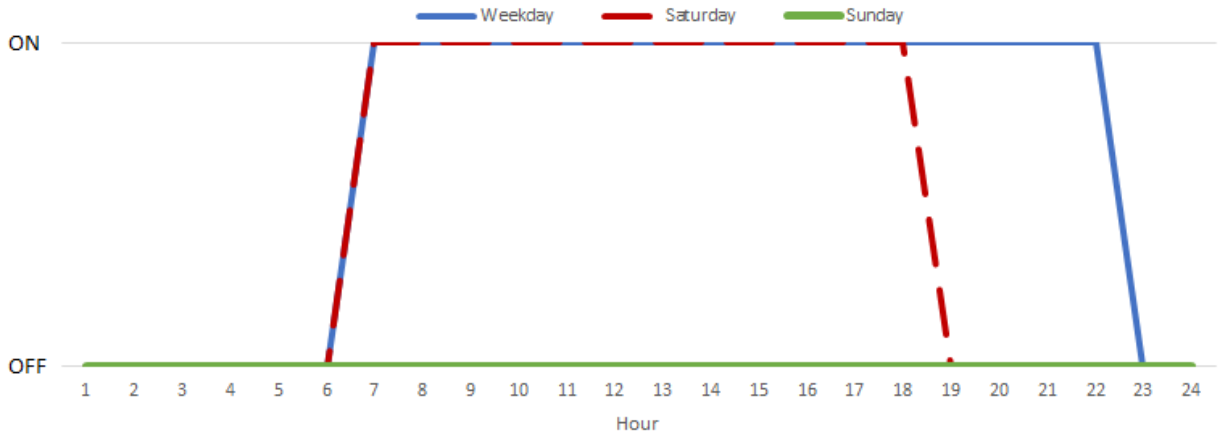
Enthalpy Wheel Effectiveness	75 %
Occupancy	
Occupant Density	10 m^2/person
Occupancy Schedule (ASHRAE, 2017c)	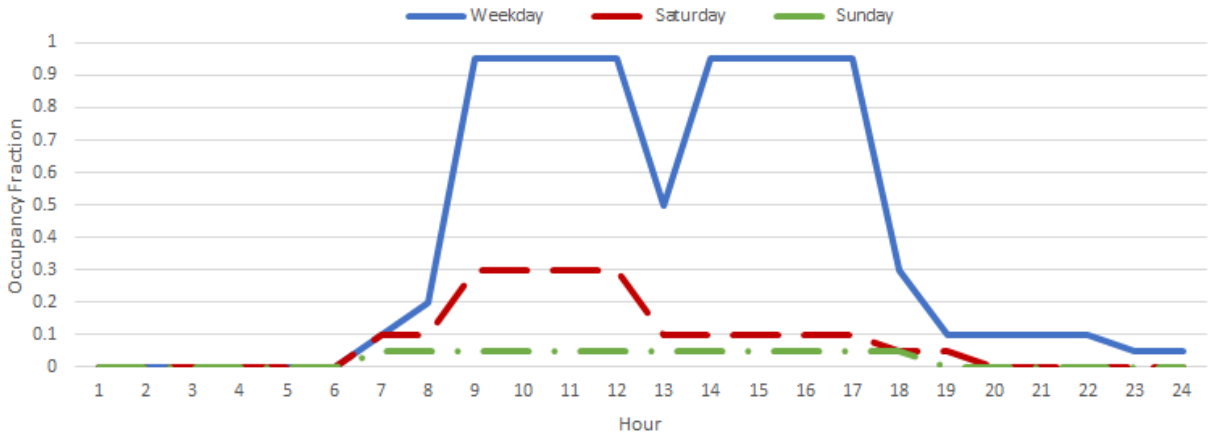
People Latent Load	45 W/person, seated light office work (ASHRAE, 2017a)
Ventilation Rate	8.5 L/s · person (0.01 kg/s · person), combined rate for office space (ASHRAE, 2016)

Assumptions, listed in Table 2.1, were made for the geometry and operation of the office building to calculate the expected loads. It was assumed that any newly constructed building would be sufficiently airtight that the latent load due to infiltration would be negligible relative to the ventilation and occupant load sources.

The Outside Air Humidity Ratio (OAHR) is the hourly humidity ratio of the outside air. If the outside air is dry, no dehumidification is needed, but if it is above some threshold, $\mathrm{OAHR_{cap}}$, dehumidification is needed to maintain thermal comfort.

To find this threshold, the internal latent load was first calculated. The $\mathrm{OAHR_{cap}}$ is lower than the thermal comfort limit to compensate for this internal load such that the mixture of ventilation air and room air is comfortable. In an office space, the main internal moisture source is water vapor from the occupants. The people latent load was used to find the amount of moisture that each occupant added to the space.

$$\begin{aligned} \text{Moisture Added} &= \frac{\text{People Latent Load}}{\mathrm{h_{fg,water}}} \\ &= \frac{45\,\mathrm{W/person}}{2500\,\mathrm{kJ/kg}} \\ &= 18 \times 10^{-6}\,\mathrm{kg/s \cdot person} \end{aligned} \tag{2.1}$$

The people latent load is diluted by the ventilation air. If fresh air is brought in at a low rate, it would need to be dry to compensate for the slow dilution of the room air. If it is brought in at a fast rate, it could be closer to the thermal comfort limit and still produce comfortable mixed air because of the faster dilution.

Thus, the $\mathrm{OAHR_{cap}}$ is found from the GCM thermal comfort limit, the latent load from the occupants, and the ventilation rate, as shown in Equation 2.2. This cap is shown as the allowable OAHR limit in Figure 2-1.

$$\begin{aligned} \mathrm{OAHR_{cap}} &= \text{Thermal Comfort Limit} - \frac{\text{Moisture Added}}{\text{Ventilation Rate}} \\ &= 0.010\,\mathrm{kg/kg} \end{aligned} \tag{2.2}$$

The EnergyPlus weather file for Boston Logan International Airport was loaded into

the Grasshopper environment. The Ladybug Humidity Ratio component (Roudsari and Pak, 2013) was used to calculate the hourly OAHR values from the drybulb and dewpoint temperatures in the weather file. Whenever the OAHR exceeds the room humidity ratio cap, 0.012 kg/kg, the supply air is assumed to pass through an enthalpy wheel to reject some of the moisture in the supply air to the less humid exhaust air, reducing the cooling needed. The enthalpy wheel was assumed to have an effectiveness, ϵ, of 75%.

The calculation below for the reduced Supply Air Humidity Ratio (SAHR) assumes that the exhaust air is at the room humidity ratio cap and that the supply and exhaust air flow rates are equal. If the OAHR is less than the room humidity ratio cap, then it cannot reject any moisture to the exhaust air, so the enthalpy wheel is bypassed and the SAHR is equal to OAHR.

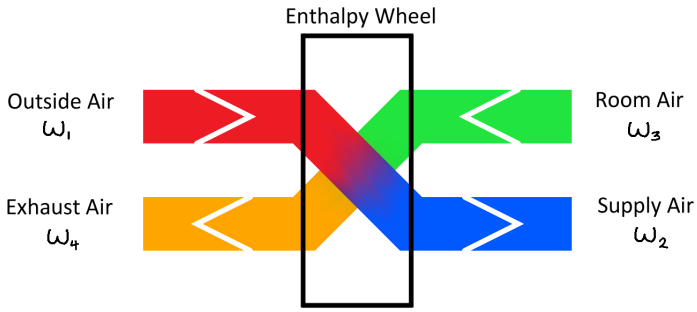

$$\epsilon = \frac{\omega_1 - \omega_2}{\omega_1 - \omega_3} \tag{2.3}$$

$$\omega_2 = \omega_1 - \epsilon(\omega_1 - \omega_3) \tag{2.4}$$

Figure 2-3: Diagram of airflows passing through enthalpy wheel

If the SAHR is below the OAHR cap, no load is calculated because the ventilation air alone is sufficient to maintain the thermal comfort of the room. No load is calculated when the HVAC equipment is off, even if there are occupants in the building, because there is no equipment running to supply ventilation air. For all other scenarios, an hourly load is calculated as shown below based on the ventilation needed for the number of occupants that hour.

$$\text{People} = \text{Area} \cdot \text{Occupant Density} \cdot \text{Occupancy Schedule Fraction} \tag{2.5}$$

$$\text{Latent Load} = \text{People} \cdot (\text{SAHR} - \text{OAHR}_{\text{cap}}) \cdot \text{Ventilation Rate} \cdot \text{h}_{\text{fg,water}} \tag{2.6}$$

2.3 Latent Load Results

The calculation method was used to calculate the loads for 1 floor. The results for the building were found by multiplying the floor results by the number of floors, 25. This assumes that all floors are identical, representing a worst-case scenario of no load diversity. The hourly latent cooling demands for the building are shown in Figure 2-4. To find the cooling consumption, the demand was assumed to be constant over the hour, so the load was simply multiplied by 3600 s. The average values are calculated as averages over the 906 hours when there is a load present. The results produced are summarized in Table 2.2.

Table 2.2: Latent Cooling Load Summary

	One Floor	Whole Building
Maximum Demand (kW)	13.7	342
Average Demand (kW)	4.07	102
Maximum Consumption (MJ)	49.2	1230
Average Consumption (MJ)	14.7	366
Total Consumption (GJ)	13.3	332

2.4 PMV Thermal Comfort Alternative

As mentioned in Section 2.1, thermal comfort is achievable for humidity ratios above 0.012 kg/kg. However, the Analytical Comfort Zone Method must be used to determine the limits of acceptable thermal environments (ASHRAE, 2017b). Acceptable thermal conditions produce a PMV within ± 0.5 using this method. The CBE Thermal Comfort Tool (Hoyt et al., 2019) is a commonly used thermal comfort calculation tool that takes in air speed, metabolic rate, and clothing insulation input values and calculates an acceptable range of operative temperatures and humidity ratios. Using the expanded thermal comfort range produced by this tool can provide a humidity ratio limit that is higher than the GCM limit.

A metabolic rate of 1 met was entered, consistent with the seated, light office work assumed in Section 2.2 (ASHRAE, 2017a). The occupants were assumed to be wearing typical office attire - trousers and a long-sleeved shirt - for a clothing level of 0.61 clo (ASHRAE,

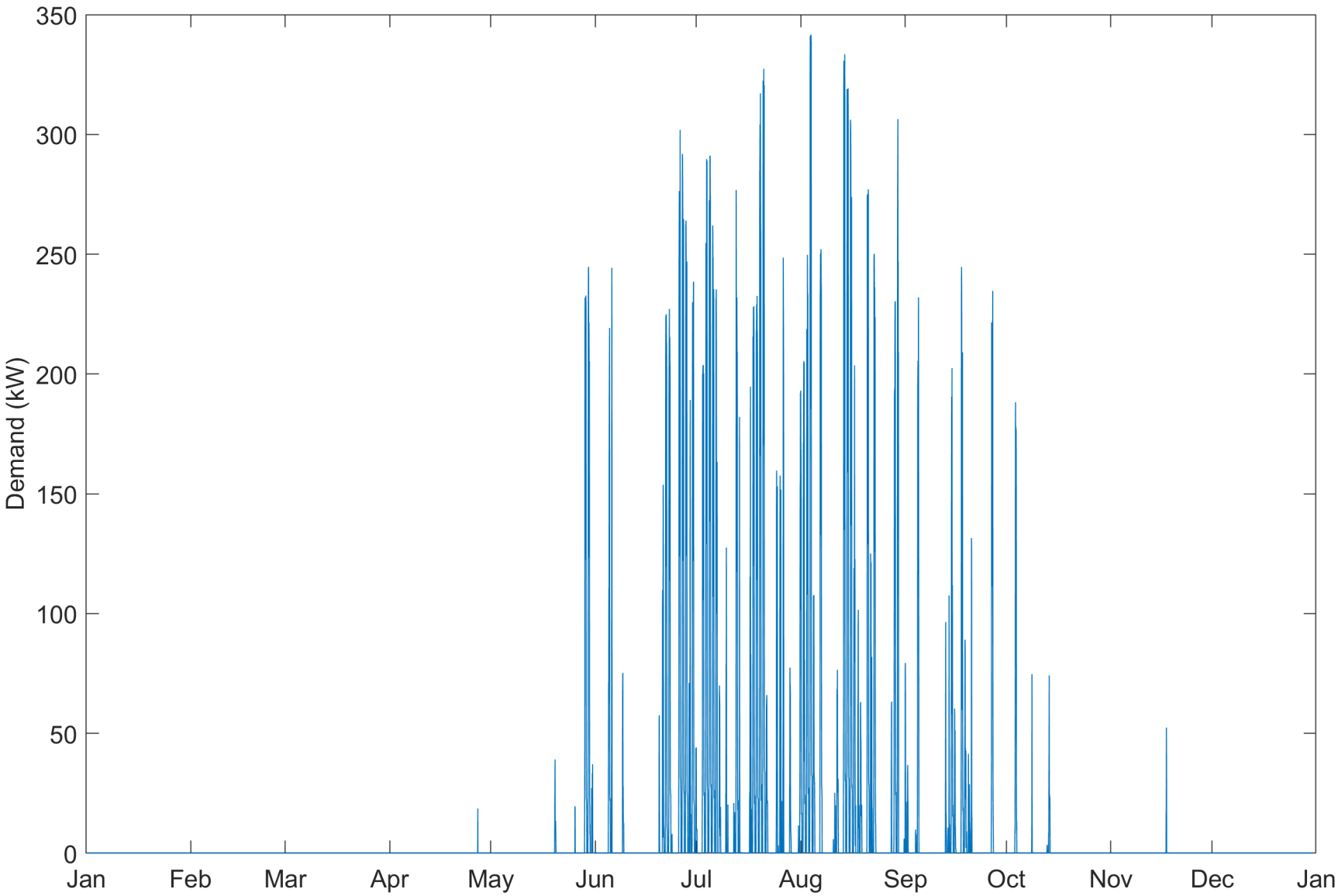

Figure 2-4: Hourly latent cooling demand of entire office building calculated from weather data

2016). The air-speed and operating temperature values were left as their default values of 0.1 m/s and 25 °C respectively.

If the air temperature is capped at 25 °C to be consistent with the operating temperature input, and comfort is maximized by targeting a PMV of 0, comfort is achieved with a humidity ratio cap of 0.014 kg/kg. The number of hours when there is a load and the amount of dehumidification needed to reach the new humidity limit is reduced, which is reflected in the reduced demand and consumption values in Table 2.3. This is also shown in the comparison of the peak latent cooling demand values for each day, shown in Figure 2-5.

The significant difference in the loads calculated by these two methods shows the large impact of thermal comfort setpoints. However, it must be acknowledged that the assumptions used for the CBE Thermal Comfort tool inputs are dependent on building details that can vary significantly between designs. Therefore, the higher loads from the GCM were chosen for designing the proposed system to meet the needs of a typical office building without imposing any further design assumptions. The resultant system sizing will likely be oversized for most office building designs, but this was deemed preferable than sizing to the less conservative PMV loads.

Table 2.3: GCM and PMV Humidity Limits Cooling Load Summary

	GCM	PMV
Number of Load Hours	906	506
Maximum Demand (kW)	342	287
Average Demand (kW)	102	88
Maximum Consumption (MJ)	1230	1033
Average Consumption (MJ)	366	317
Total Consumption (GJ)	332	160

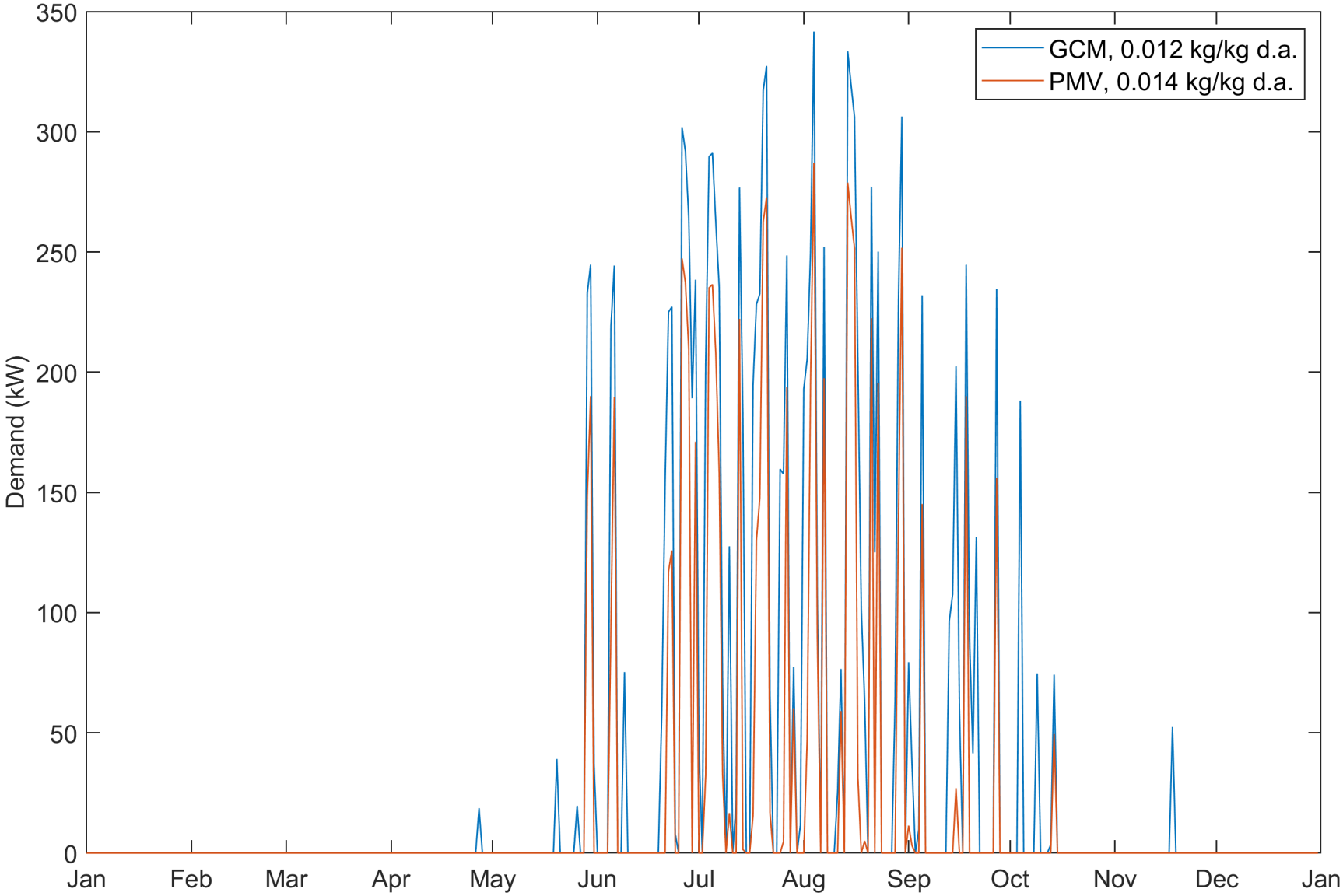

Figure 2-5: Daily maximum latent cooling demand values for GCM and PMV humidity limits

Chapter 3

System Sizing

As a preliminary test, rough calculations were used to size the design of the proposed system based on the latent loads found in the previous chapter. If the size of the soil block or the number of pipes needed was infeasibly high, then the system would be difficult and costly to install. However, if these values were found to be reasonable, the system design would be worth further investigation.

3.1 Assumed Material Properties

The soil properties in VolpeMIT development area were not known exactly, so estimated values were used in these calculations and in subsequent modeling (Engineering ToolBox, 2003, 2010). As the VolpeMIT development is located on reclaimed land, it was assumed that the soil would be saturated. Wet soil properties are favorable for the performance of this system because water has a high specific heat capacity, allowing for greater thermal storage than dry soil. If the actual VolpeMIT soil was found to be drier than assumed, the soil could perhaps be wetted during the system installation to align it with the properties in Table 3.1. In some cases, the wet soil could freeze during winter charging, increasing its effective heat capacity. As a conservative estimate, freezing was not included in the heat capacity of the soil.

Water properties were interpolated for 5 °C water (Incropera and DeWitt, 2002). The values used are listed in Table 3.2. During winter charging, the water temperature starts

Table 3.1: Thermophysical properties of soil

Density, ρ_s	$1600\,\mathrm{kg/m^3}$
Heat Capacity, $c_{p,s}$	$1480\,\mathrm{J/kg \cdot K}$
Thermal Conductivity, k_s	$2.4\,\mathrm{W/m \cdot K}$
Thermal Diffusivity, α	$2.368 \times 10^6\,\mathrm{m^2/s}$

at the ambient soil temperature and reaches 0 °C only when charging is completed. During summer discharging, it is unclear how much the water temperature will rise over the season and how quickly that will occur. Therefore, 5 °C was used an estimate average temperature for the expected range of water temperatures.

Table 3.2: Thermophysical properties of water

Density, ρ_w	$1000\,\mathrm{kg/m^3}$
Specific Heat Capacity, $c_{p,w}$	$4200\,\mathrm{J/kg \cdot K}$
Viscosity, μ	$1500 \times 10^{-6}\,\mathrm{N \cdot s/m^2}$
Thermal Conductivity, k_w	$0.6\,\mathrm{W/m \cdot K}$
Prandtl Number, Pr	11

3.2 Soil Volume

To dry the air, the dehumidification system would need to cool the air down to the dewpoint temperature for a humidity ratio of 0.010 kg/kg. This is 14.4 °C under standard atmospheric pressure. The water temperature used to supply the system would have to be cooler than the dewpoint limit, so it was assumed that the highest allowable water temperature would be 10 °C. As the soil is used to cool the water in summer, the soil temperature must remain lower than the water temperature. Therefore, the soil also has a highest allowable temperature of 10 °C. The minimum soil temperature was taken as 0 °C from the freezing point of water. Therefore, the maximum change in soil temperature was estimated as $\Delta T = 10\,^\circ\mathrm{C}$.

The mass of the soil block needed to satisfy the total building latent cooling consumption can be found using an energy balance. As we are proposing that they system is installed by excavating the soil block when forming the foundation of the building, the soil block was assumed to have the same footprint as the building itself. Thus, the height of the soil block

can be determined from the overall volume required.

$$Q = m_s c_{p,s} \Delta T = 332\,\text{GJ} \tag{3.1}$$

$$m_s = 22.4 \times 10^6\,\text{kg} \tag{3.2}$$

$$V_s = \frac{m_s}{\rho_s} = 1400\,\text{m}^3 \tag{3.3}$$

$$H_s = \frac{V_s}{W_s \cdot L_s} = 7.96\,\text{m} \tag{3.4}$$

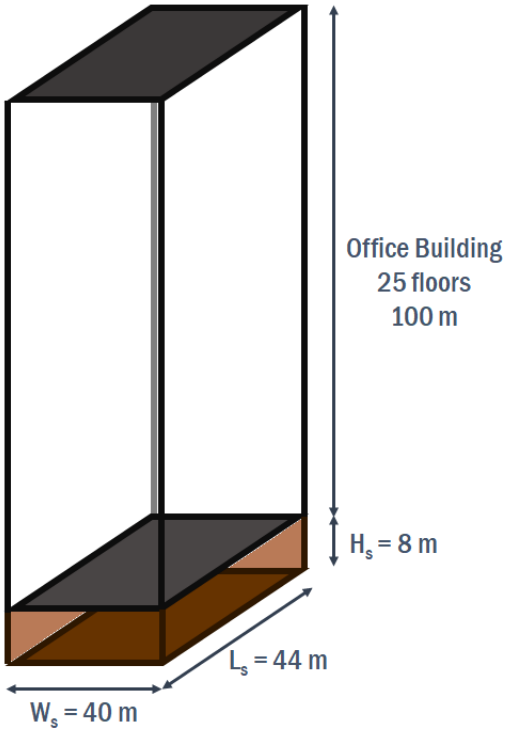

Figure 3-1: Dimensions of soil block relative to office building served

As the additional depth was roughly equivalent to adding two basement floors to the building, the excavation needs did not seem excessively deep. Although Figure 3-1 shows the soil block directly beneath the building, it should be noted that there would be some space between them. This spacing is needed to provide room for the building foundation and to avoid direct thermal conduction between the block and the building. However, this spacing is unlikely to make the total excavation depth unreasonably high and so, the volume

of soil needed to contain the building latent load is not a barrier to system feasibility.

3.3 Pipe Spacing

The spacing between pipes in the soil blocks affects the ability of the soil block to reach 0 °C within the 3-month charging period. If a large number of pipes is used to carry 0 °C water through the block, it is assured that the soil will cool down to 0 °C in time, but at the cost of piping and pump power. Furthermore, this reduces the volume of actual soil available for storing the load. If too small a number of pipes is used, the soil will not cool down fast enough, lessening the load that could be rejected to the block in the summer.

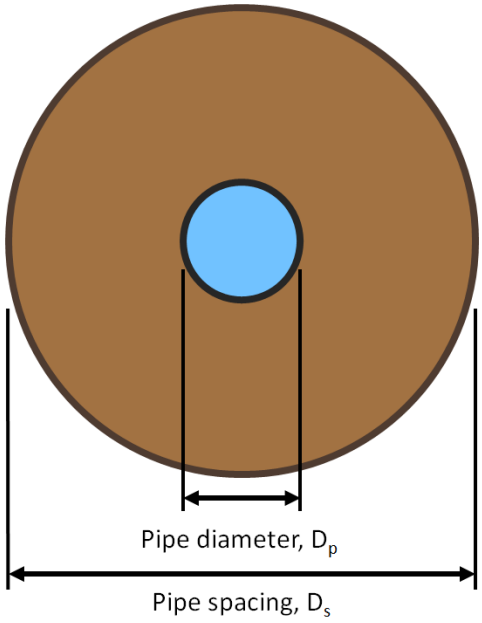

Figure 3-2: Soil and pipe dimension nomenclature

The number of pipes in the soil block was found from the pipe spacing, assuming a rectangular grid of pipes. A different packing method could increase the number of pipes available but would impact the boundary condition assumptions used for the transient heat transfer model in Chapter 4. The pipes were evaluated as cylindrical systems with heat transfer in the radial direction only, neglecting axial temperature gradients. In steady-state

conditions, the governing equation for the heat transfer in the pipe simplifies to

$$\frac{1}{r}\frac{d}{dr}(kr\frac{dT}{dr}) = 0\,. \tag{3.5}$$

The rate of conduction across the pipe-soil boundary can be expressed as

$$q = -k_s A_p \frac{dT}{dr} \tag{3.6}$$

where A_p is the surface area of the pipe. Averaging the total latent load over the 3 month charging period for q, using ΔT for dT, and using $D_s/2$ for dr simplifies Equation 3.5 to find the total pipe surface area needed for winter charging. The diameter of each pipe, D_p can then be found from the total pipe surface area and number of pipes. These dimensions are illustrated in Figure 3-2. The values of n_p, A_p, and D_p calculated for several values of D_s are shown in Table 3.4.

$$\begin{aligned} q &= \frac{\text{Building annual latent consumption}}{\text{3 months}} \\ &= 42.7\,\text{kW} && (3.7) \\ n_p &= \frac{W_s}{D_s} \times \frac{H_s}{D_s} && (3.8) \\ A_p &= \frac{qD_s}{2k_s\Delta T} && (3.9) \\ D_p &= \frac{A_p}{n_p \pi L_p} && (3.10) \end{aligned}$$

3.3.1 Water Flow

Similar to the soil block sizing method, the mass flow of the water through the pipes is found using an energy balance with the latent load averaged over the charging period. As with the soil block, the expected ΔT of the water is 10 °C. From this, the speed of the water flow and the associated Reynolds number can be found for all pipe diameter options. To be conservative, the flows were calculated to meet the peak building latent cooling demand, 342 kW, when the necessary flowrate would be at its fastest.

$$q = \text{Peak building latent demand} = 342\,\text{kW} \tag{3.11}$$

$$\dot{m}_w = \frac{q}{c_{p,w}\Delta T} \tag{3.12}$$

$$u = \frac{4\dot{m}_w}{n_p \rho_w \pi {D_p}^2} \tag{3.13}$$

$$\text{Re}_D = \frac{\rho u D_p}{\mu} \tag{3.14}$$

3.3.2 Piping Pressure Drop

The total pressure drop from the piping in the soil block is caused by pipe fittings and friction along the pipe. This relationship is described by

$$\Delta P = \Delta P_{\text{friction}} + \Delta P_{\text{fittings}} \tag{3.15}$$

$$\Delta P_{\text{friction}} = \frac{1}{2}\,\rho u^2\,\frac{fL}{D_p} \tag{3.16}$$

$$\Delta P_{\text{fittings}} = \frac{1}{2}\,\rho u^2\,\Sigma K \tag{3.17}$$

where f is the friction factor and K is the fitting coefficient. For fully-developed laminar flow, $\text{Re}_D < 2300$, the friction factor is

$$f = \frac{64}{\text{Re}_D}. \tag{3.18}$$

The pipes in the soil block are headered together with tees and 90 deg elbows. Using a pipe spacing of D_s, there are $40/D_s$ pipes per horizontal layer and $8/D_s$ layers in the soil block. In each layer, 2 of the pipes will have elbows at both ends and the rest of the pipes will have tees at both ends. Therefore, the number of tees and elbows in each soil block is

$$\text{Number of tees} = 2 \cdot \frac{8}{D_s} \cdot \left(\frac{40}{D_s} - 2\right) \tag{3.19}$$

$$\text{Number of elbows} = 4 \cdot \frac{8}{D_s} \tag{3.20}$$

Table 3.3: Pipe fitting pressure drop coefficients, K

Fitting	K
90 deg elbow, long radius:	0.6
Tee, flow through branch:	1.8

The ASHRAE Handbook gives the values listed in Table 3.3 for the pressure drop coefficients, K, of the pipe fittings used (ASHRAE, 2017a).

The pump energy needed to overcome this pressure drop is calculated as

$$w_p = \dot{V}_w \Delta P \ . \tag{3.21}$$

3.3.3 Pipe Spacing Comparison

Table 3.4: Piping dimension and water flow comparison results

Pipe spacing, D_s (m)	**1**	**2**	**4**
Number of pipes, n_p	320	80	20
Total pipe surface area, A_p (m^2)	28,471	14,236	7,118
Pipe diameter, D_p (cm)	8.85	17.7	35.4
Peak water flow results			
Mass flow per pipe, $\dot{m}_{w,p}$ (kg/s)	0.03	0.10	0.41
Water flow speed, u (m/s)	0.004	0.004	0.004
Reynolds number, Re_D	244	488	976
Friction pressure loss, $\Delta P_{\text{friction}}$ (Pa)	1.02	0.25	0.06
Fittings pressure loss, $\Delta P_{\text{fittings}}$ (Pa)	9.53	2.30	0.53
Peak pump energy, w_p (W)	0.086	0.021	0.005

The results shown in Table 3.4 were calculated for a range of pipe spacings that were considered reasonable for the soil block. The 1 m pipe spacing is a poor option because it requires a large number of pipes and uses the most pump energy. In contrast, the 4 m pipe spacing option requires few pipes and uses very little pump energy, but needs a pipe diameter that is larger than standard, which could substantially impact its cost. Ultimately, the 2 m pipe spacing was chosen as it produces the best balance between number of pipes and pipe diameter.

3.4 Soil Block Dimension Summary

To summarize the findings from the previous calculations in this chapter, the selected dimensions of the soil block and piping for the proposed system design are given in Table 3.5. The pipe diameter of 17 cm is slightly different than the value of 17.7 cm calculated previously. This smaller diameter was a holdover from a previous iteration of the calculations. The older value had already been implemented in the MATLAB modeling in the following chapters, but as the difference was small, it was not considered necessary to switch to the new value.

Table 3.5: Soil block and piping dimensions

Soil block	
Width	40 m
Length	44 m
Height	8 m
Piping	
Spacing, D_s	2 m
Diameter, D_p	0.17 m

Chapter 4

Winter Modeling

The average outdoor air temperature between December and February is $-0.4\,^{\circ}\mathrm{C}$, which is much lower than the dewpoint temperature of the dehumidification setpoint, $14\,^{\circ}\mathrm{C}$. Conventional chiller systems are inefficient at serving latent loads because of the cold water temperatures needed for dehumidification. If the freely available cold weather can be used during this period to charge the soil block, the proposed system can produce sufficiently cold water in summer with just pumping energy, making it far more efficient than conventional vapor-compression systems.

4.1 Pipe and Soil Blocks

To evaluate the performance of this winter charging, a transient heat transfer model was created in the MATLAB Partial Differential Equation (PDE) toolbox (MATLAB, 2018). To simplify modeling, a pipe block consisting of one 40 m pipe in a 2 m diameter layer of soil was simulated to represent the heat transfer in the soil block. The majority of the pipes lie within the center of the soil block and would see identical heat transfer conditions as they are given the same mass flows and entering temperatures of water. The symmetry on either side of the boundaries surrounding the pipe block would result in no net heat transfer, so they can be assumed to have adiabatic boundaries. The pipe blocks along the edge of the soil block are dependent on the conditions of the soil surrounding the block, which would significantly increase the complexity of the model. To avoid interacting with

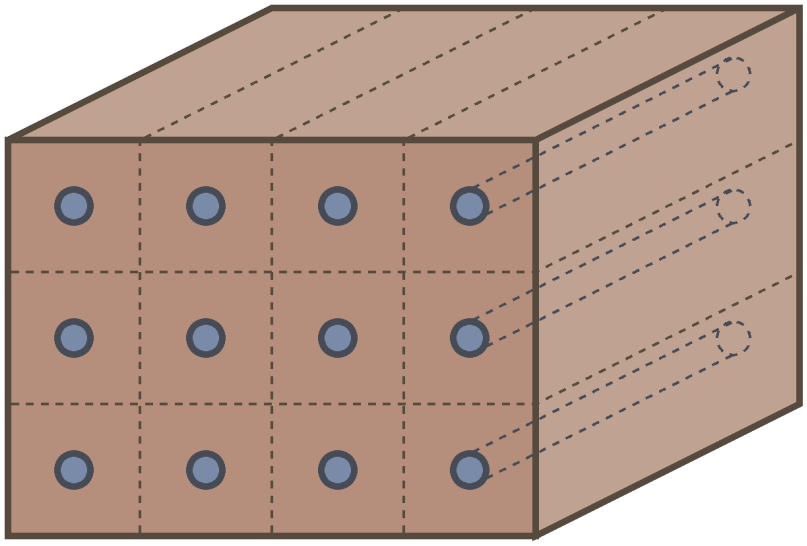

Figure 4-1: Soil block consisting of component pipe blocks

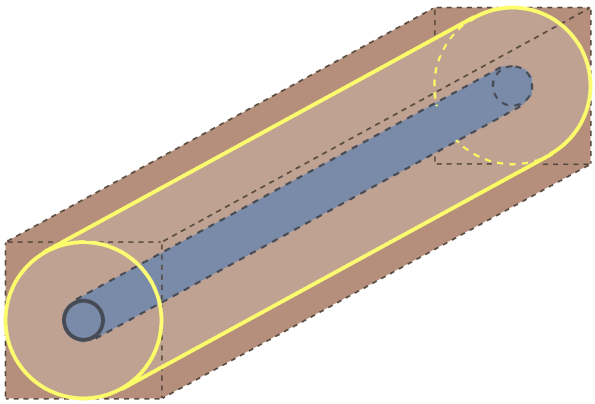

Figure 4-2: Pipe block, modeled as cylinder

the surroundings, the soil block could potentially be installed with a layer of insulation to provide an adiabatic boundary to the entire block. For a feasibility study, the modeling of a single interior pipe block was considered sufficient to represent the performance of the entire soil block, including the edge cases. The soil around the pipe was modeled as a circular

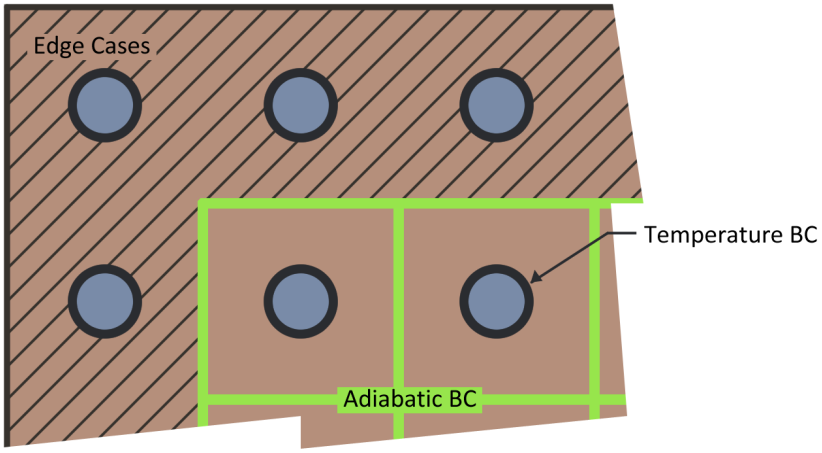

Figure 4-3: Boundary conditions in soil block

cylinder, rather than a square, to simplify the model and reduce simulation time. The omitted area makes up 21.5% of the total square area. A supplemental model was created with an equivalent diameter such that the amount of soil in each circular slice was equal to the soil in the square cross-section. The results of this model are discussed in Section 4.6.1.

$$A_{square} = A_{circle,\,eq} \tag{4.1}$$

$$D_{soil}{}^2 = \frac{\pi}{4} D_{eq}{}^2 \tag{4.2}$$

$$D_{eq} = \frac{2}{\sqrt{\pi}} D_{soil} = 2.3\,\text{m} \tag{4.3}$$

4.2 Soil Slices

A pipe block is modeled as nine cross-sectional 2D slices spaced 5 m apart along its 40 m length. The spacing of these slices can be seen in Figure 4-6. It was assumed that heat transfer in the axial direction along the pipe length is negligible relative to the radial variation. Each slice is modeled separately and has a unique radial temperature variation based

on the pipe water temperature boundary condition it sees. The conductive resistance of the pipe material is considered negligible relative to the conductive resistance of the soil, so it is not included in the model.

As shown in Table 3.4, the mass flow needed was found to be very low. In order to simulate this correctly, the model timestep must be reduced, which in turn significantly increases the time needed to simulate a three-month period. As the pump energy is unlikely to be large, it was simpler to increase the flow rate through the pipe to 0.5 kg/s. At this flow rate, the water speed is still low, $u = 0.2\,\mathrm{m/s}$, and the Reynolds number is still laminar, $\mathrm{Re}_D = 2500$. The laminar flow confirms that the resultant pump energy increase will be small and that the convective resistance of the water flow is negligible in comparison to the conduction resistance. Therefore, the increased flow rate simplifies the simulation at little cost to the overall energy use and the boundary condition assumptions.

The MATLAB PDE toolbox solves the transient heat equation

$$\frac{\partial T}{\partial t} = \alpha \frac{1}{r} \frac{\partial}{\partial r}\left(r \frac{\partial T}{\partial r}\right) \tag{4.4}$$

with a timestep of 200s for the nodal temperatures of the slice. Equations 4.5 and 4.6 are applied as boundary conditions at the pipe and soil boundaries respectively, highlighted in Figure 4-4. The initial condition is given by Equation 4.7.

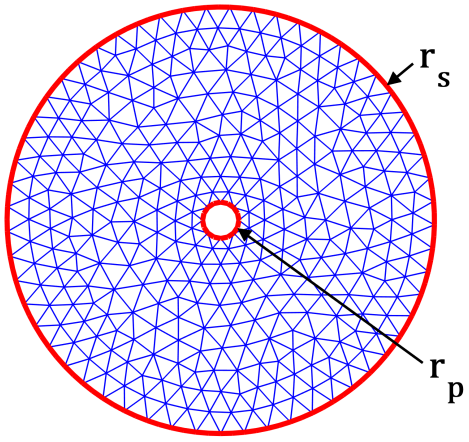

Figure 4-4: Slice model mesh with annotations indicating locations of the soil boundary, r_s, and pipe boundary, r_p

$$T(r_p, t) = T_w(t) \tag{4.5}$$

$$\frac{dT(r_s, t)}{dr} = 0 \tag{4.6}$$

$$T(r, t = 0) = 10 \tag{4.7}$$

4.3 Initial Soil Temperature

The dewpoint temperature associated with the maximum allowable OAHR, 0.010 kg/kg, is about 14 °C (see Figure 2-1). The water temperature in the dehumidifier should be lower than this temperature for the air to be cooled to the dewpoint. Therefore, it was assumed that the dehumidifier water would generally stay below 10 °C. As the soil temperature is inherently tied to the water temperature, this is also the expected maximum soil temperature.

Right after installation, the soil block might be warmer than 10 °C due to greater exposure to outdoor conditions during construction, increasing the amount of cooling needed to charge the block in winter. This problem could be further exacerbated depending on the timing of the system installation. However, the scope of this study is to examine the general feasibility of the system, so the soil block was assumed to start at a uniform temperature of 10 °C. As the system is used over the years, the impact of this initial warmth should diminish, making the maximum soil assumption more valid.

The soil block initial temperature is also tied to variations in the annual latent load. A year with mild cooling loads might not need the full cooling potential of the block, leaving it at an average temperature that is lower than 10 °C. Conversely, an unusually humid summer could drive soil temperatures above 10 °C towards the 14 °C dewpoint temperature limit such that even more charging is needed during the following winter. This is a potential ΔT of at most 4 °C. Therefore, on average, the initial temperature assumption of 10 °C is likely to be correct.

4.4 Water Temperatures

The temperature of the water entering the pipe block at Slice 1 is constant at 0 celsius during the entire charging period based on the assumption that the cooling source can consistently provide cold water during this period. Therefore, Slice 1 is modeled with a constant temperature pipe boundary condition, $T_w(t) = 0$. The cooling source performance will be discussed in further detail in Chapter 6.

Once Slice 1 has been modeled for the entire charging period, the change in radial tem-

peratures is used to determine the energy lost by the soil over each time step in the 3 month period. The energy loss of the soil is equal to the energy gain of the water and so the increase in water temperature between slices can be found. The temperature rise between slices is added to the entering water temperature of the preceding slice to get the entering water temperature of the current slice. This is applied as a time-dependent boundary condition on the inner diameter of the slice. The model proceeds in order down the pipe until all slices have been modeled for the whole charging period, as described in Figure 4-5.

r = Radial distance from midpoint of circle

$T_s(r,t)$ = Soil temperature at distance r and time t

$T_{\text{w, prev}}(t)$ = Entering water temperature for previous slice at time t

z = Spacing between slices, 5 m

$$q(t) = \rho_s c_{p,s} z \cdot 2\pi \int_{r_p}^{r_s} r T_s(r,t) dr \tag{4.8}$$

$$\Delta q(t) = q(t) - q(t+1) \tag{4.9}$$

$$\Delta T_w(t) = \frac{\Delta q(t)}{\dot{m} c_{p,w}} \tag{4.10}$$

$$T_w(t) = T_{w,prev}(t) + \Delta T_w \tag{4.11}$$

4.5 Alternative Modeling Method

Several attempts were made to simulate the soil block and water flow as a 3D model in ANSYS Fluent but these produced poor results. The largest dimension in the XY plane is 2 m but along the Z axis, it is 40 m. These disparate scales produced meshes that were either too fine with extremely long computation times, or too coarse with inaccurate results. Therefore, the 2D slicing method remains the preferred method of analysis for this stage of feasibility study.

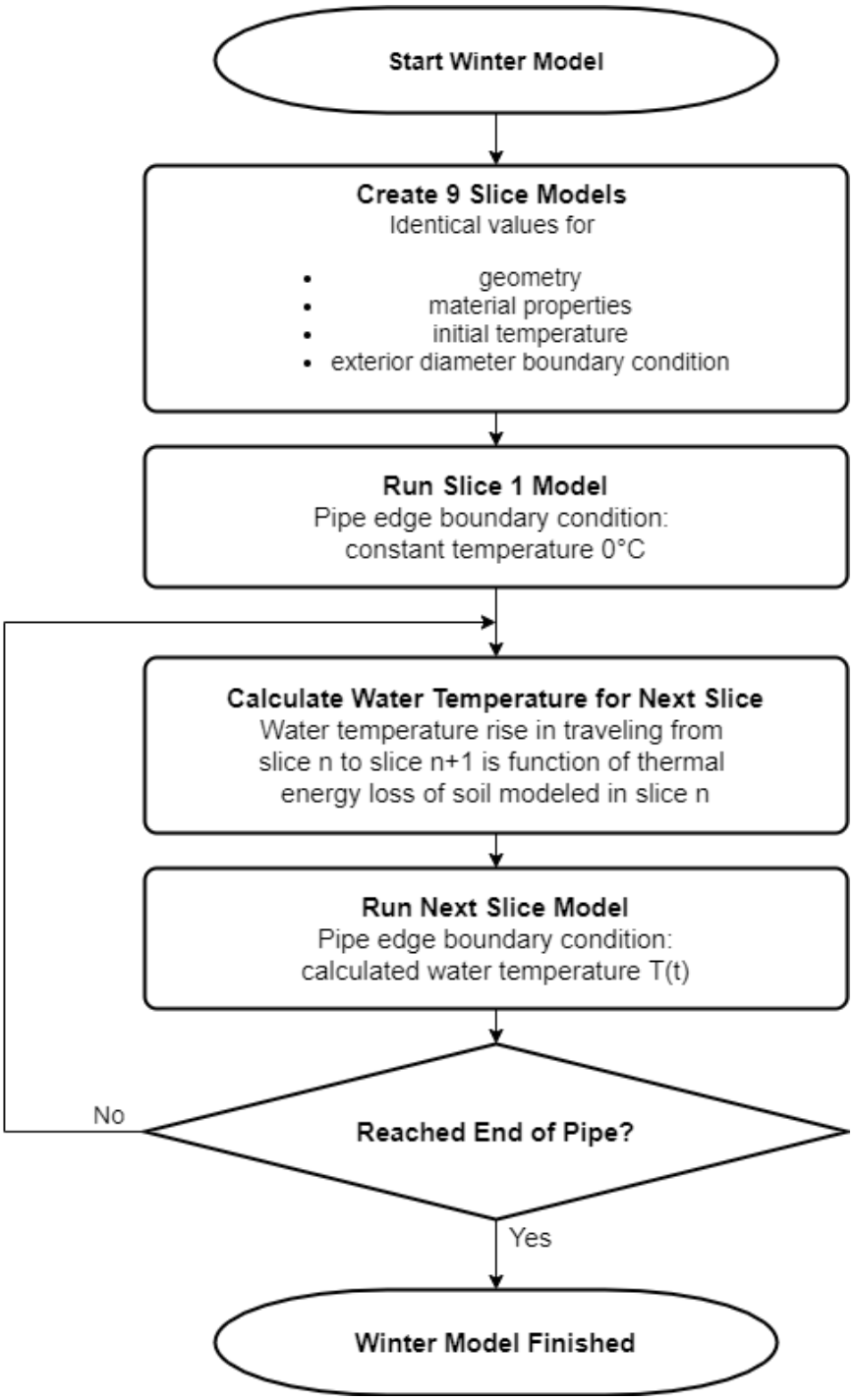

Figure 4-5: Flowchart of winter modeling program

4.6 Results

The model results show that the soil temperatures drop rapidly in the first month of charging. A log fit to the data shows that the temperatures at r_s drop by about 95% every 30 days. It should be noted that results are only shown for 5 of the 9 slices (10 m spacing) to simplify the figures. All nine slices were included in the model as shown at the top of Figure 4-6.

The axial plot of water temperatures, Figure 4-7, supports the assumption that the axial heat transfer is negligible in comparison to the radial heat transfer. By the end of the first month, the water temperature remains relatively steady as it flows through the pipe, suggesting that the soil temperature close to the pipe edge is already close to the water temperature. This is supported by the results in Figure 4-6, which show the colder temperatures radially diffusing through the slices more slowly over the charging period. At any time t, the axial temperature change of the water was found to be very modest compared to the radial temperature differences, indicating that the 2D model is a reasonable approximation for the pipe block.

The log plot Figure 4-9 shows the time taken to reach chosen temperature limits more clearly than the linear Figure 4-8. The outer edge, D_s, of slice 9 at the end of the pipe block, takes about 55 days to reach 0.1 °C. By the end of the charging period, all slices are well-under 0.01 °C at their outer soil diameters. These results prove favorable for the cooling source because it may not need to provide 0 °C water for a full 3 months. Therefore, the system could still be sufficiently charged in years with mild or short winters.

4.6.1 Equivalent Diameter Results

When D_{eq} is used to include all the soil in the pipe block, the soil volume in the model increases and the heat at $D_{s,eq}$ has farther to travel to reach the pipe. The outer soil diameter reaches 0.1 °C by day 75 but does not reach 0.01 °C by the end of the charging period. The results shown in Figure 4-10 are otherwise similar to those shown in Figure 4-9. As expected, the soil in the corners of the pipe block, which are not included in the 2 m diameter model, is warmer than the rest of the soil at the end of the charging period. However, the results show that the difference in final temperatures achieved by the two model diameters is less

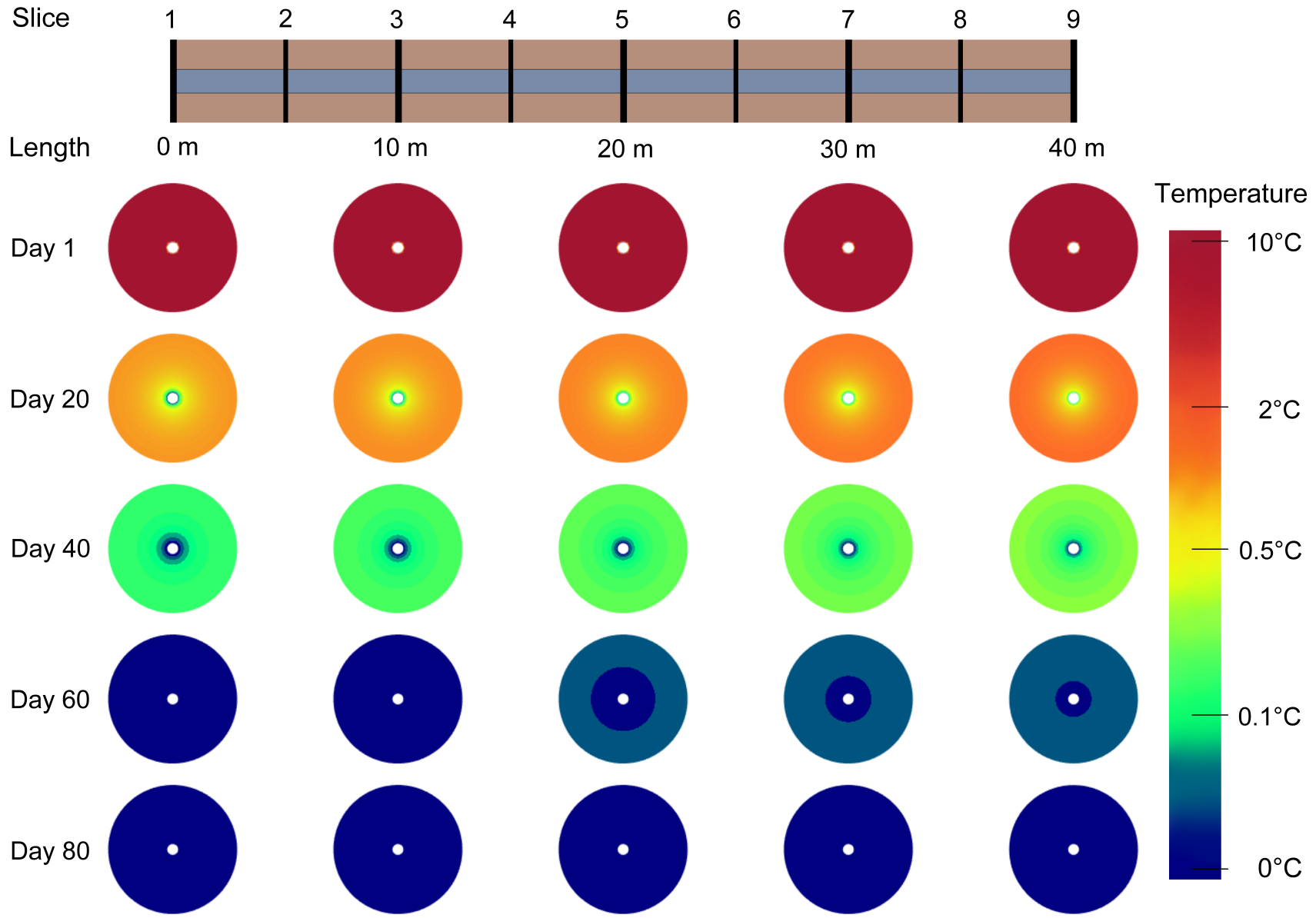

Figure 4-6: Temperatures of soil slices during charging period

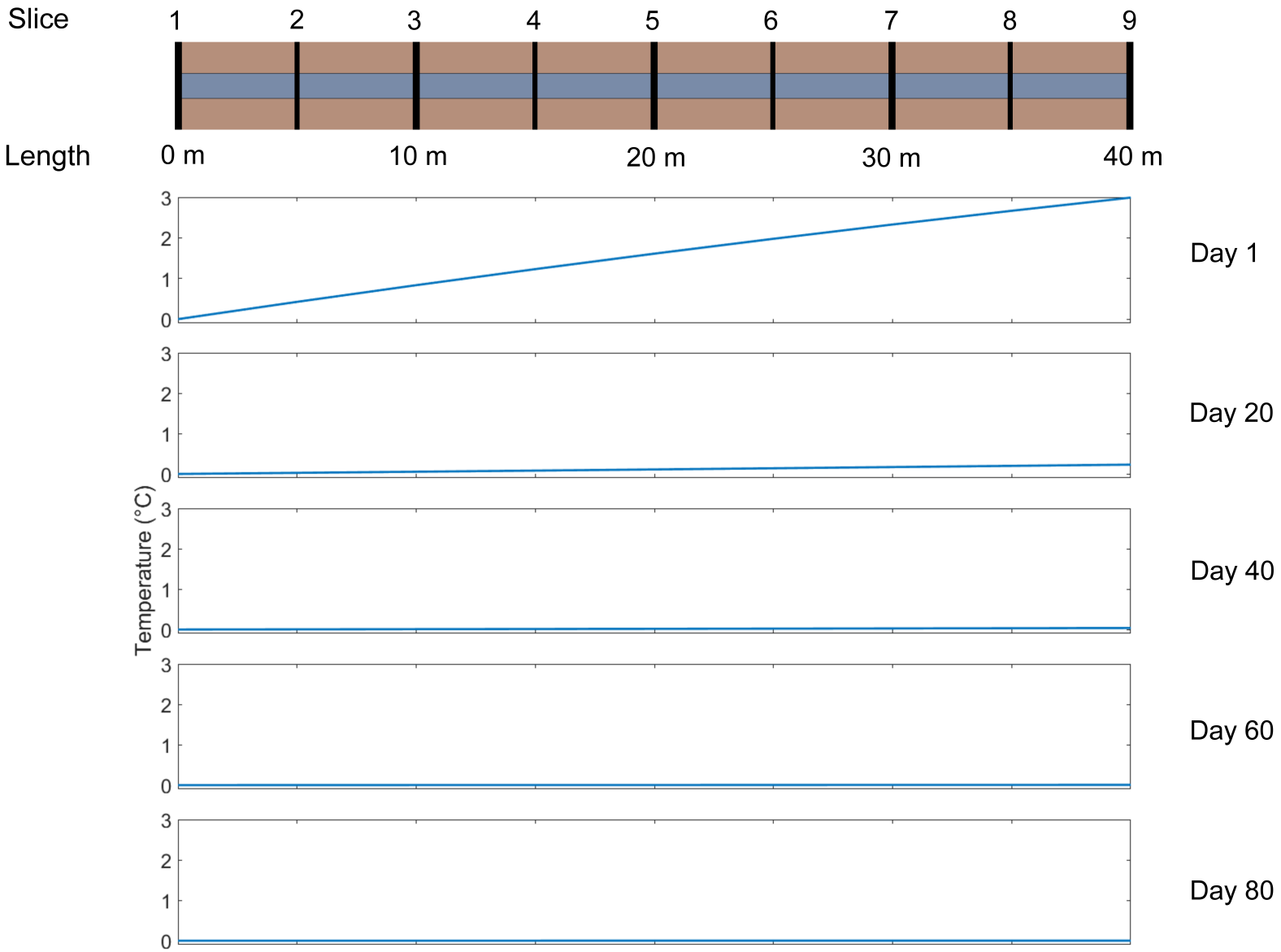

Figure 4-7: Water temperature boundary condition along pipe during charging period

than 0.1 °C, so neglecting the corners does not negate the results of the smaller diameter models.

4.7 Conclusion

The model result shows that a consistent supply of 0 °C water over a 3-month charging period was successful in cooling the pipe block. As all the pipe blocks in the soil block are assumed equal, this statement can be extended to say that the entire soil block is successfully charged. The shoulder period between winter charging and the start of the latent load demand is assumed to be an adiabatic period for the soil block as no water is passed through the system. During this time, the temperature gradients within the soil will have the chance to even out such that the soil block can be assumed to be at a uniform temperature of 0 °C at the start of the summer modeling period.

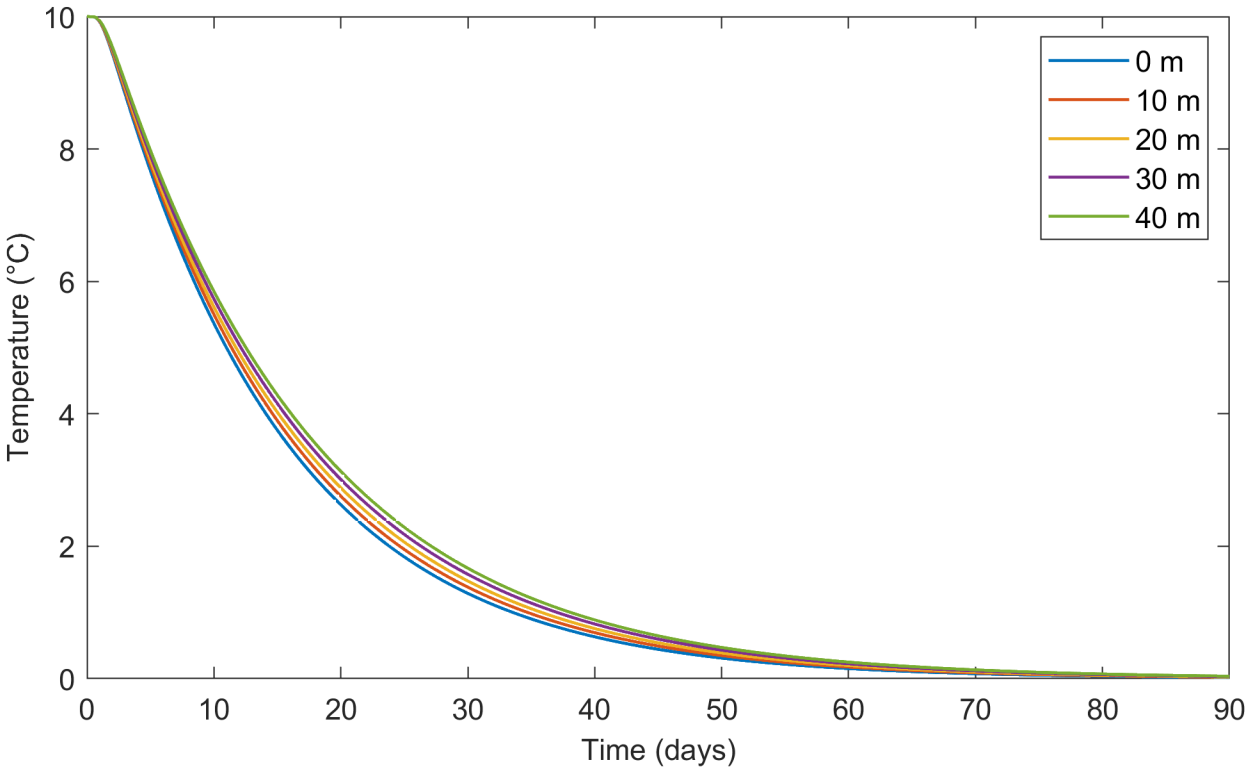

Figure 4-8: Temperature of soil block outer diameter, D_s, during winter charging

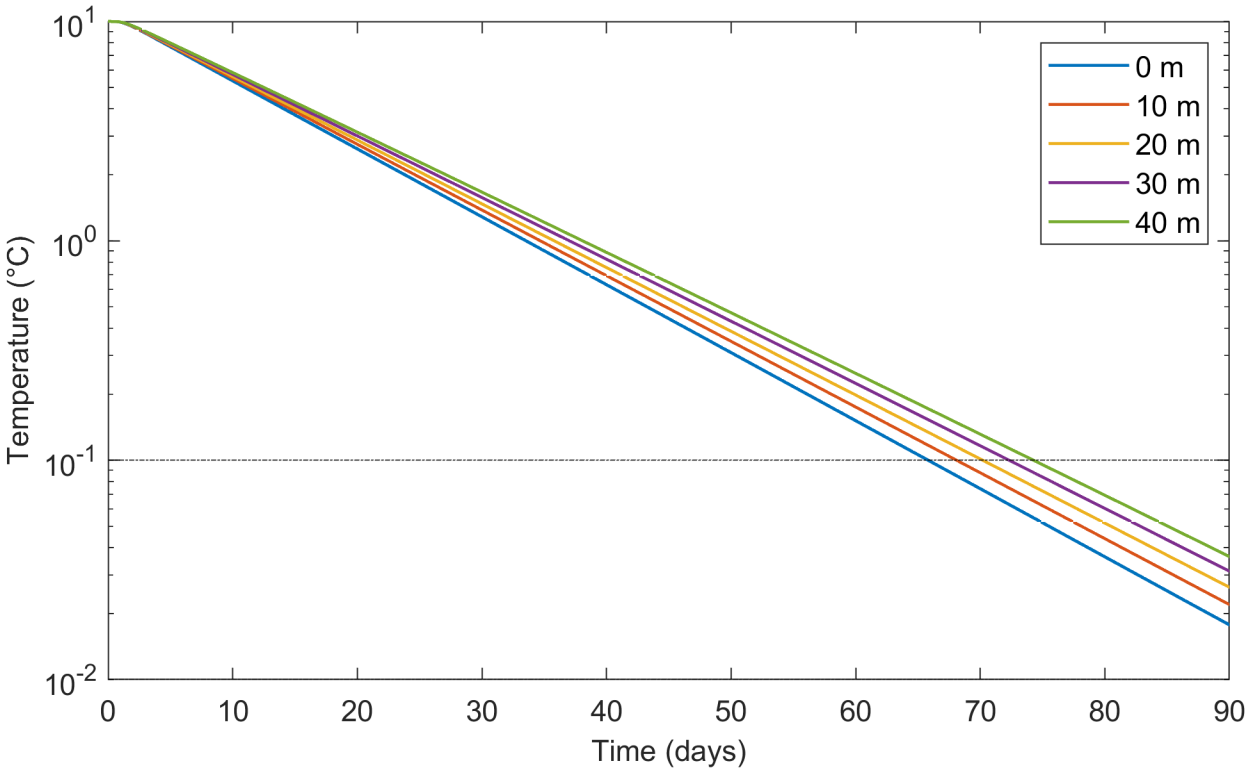

Figure 4-9: Log scale temperature of soil block outer diameter, D_s, during winter charging

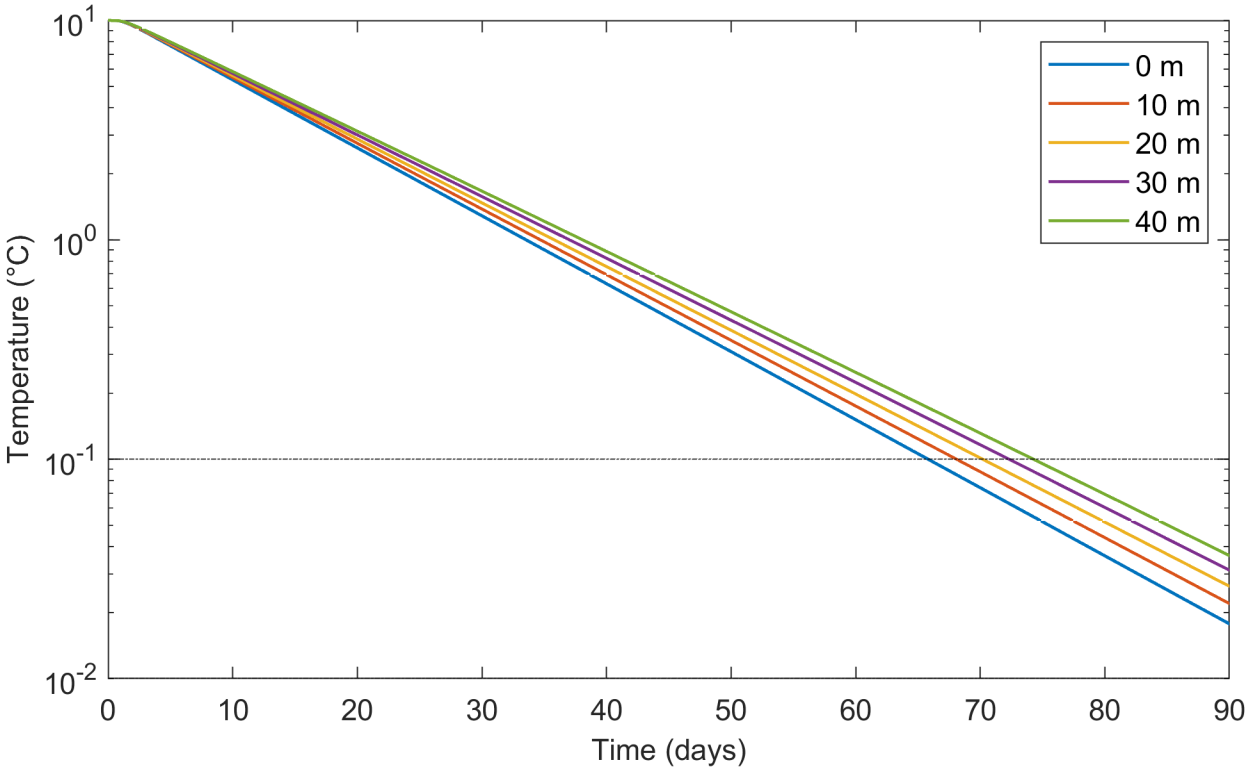

Figure 4-10: Log scale temperature of equivalent diameter, D_{eq}, during winter charging

Chapter 5

Cooling Source Options

In Chapter 4, it was assumed that there would be some form of cooling source component that could provide the cold water to charge the soil block. As the system has shown its potential in meeting the summer dehumidification loads, this assumption must be reexamined to prove that the winter charging is indeed feasible. Hence, the cooling source component must be designed and evaluated before any meaningful conclusion can be made about the overall feasibility of the system.

As mentioned in Section 1.3.2, the proposed system is considering two options: an outside air Heat Exchanger (HX) and a near-surface source loop. Yang et al. (2013) use an outdoor air HX in their design, so its precedence makes it a promising candidate for the cooling source component. However, the HX fan energy use is likely to be a significant penalty to the system performance. Therefore, the near-surface source loop is also evaluated as a fanless alternative to minimize system energy use.

5.1 Heat Exchanger

HX units are relatively straightforward to install and could be placed on the building itself, so they are an attractive option for applying this proposed system to buildings in dense areas. However, in the VolpeMIT development, where green space is included in the zoning requirements, the spatial benefits of HXs may not outweigh the impact of their energy use. The ϵ-NTU method could be used to design a hypothetical heat exchanger that could meet

an average heat transfer capacity requirement for the season. However, it was decided that using the specifications of commercial units would provide more realistic values for capacities and power use than a theoretically-designed unit.

5.1.1 Effectiveness Calculation

The commercial units from Alfa Heating Supply (nd) examined were rated for heating air with hot water, so they had temperatures differences far higher than the winter charging operation. Therefore, the rated capacities alone could not be used to estimate the commercial HX performance in this use. Instead, the data provided for the commercial units was used to estimate their effectiveness at their rated conditions. This effectiveness was assumed to be constant over all operating temperatures to analyze their performance during the winter charging. As this study is intended only to examine the general feasibility of the system, this method produces sufficiently accurate estimates.

Table 5.1: Rated properties of HTL 24x24 HX unit (Alfa Heating Supply, nd)

Water flow rate, $\dot{V}_w$	12 gpm ($7.57 \times 10^{-4}\,\mathrm{m^3/s}$)
Water-side pressure drop, ΔP_w	2.27 ft w (6.78 kPa)
Air flow rate, $\dot{V}_a$	1800 cfm ($0.85\,\mathrm{m^3/s}$)
Air-side pressure drop, ΔP_a	0.22 in w (54.7 Pa)
Capacity, q	95 007 Btu/h (27.8 kW)
Entering water temperature, $T_{\mathrm{w,\ in}}$	140 °F (60 °C)
Entering air temperature, $T_{\mathrm{a,\ in}}$	65 °F (18.3 °C)
Leaving air temperature, $T_{\mathrm{a,\ out}}$	114 °F (45.5 °C)

The HTL 24x24 model (Alfa Heating Supply, nd) was chosen as the design HX unit with rated properties as shown in Table 5.1. The effectiveness, η, of the unit is then calculated as

$$C_{\min} = \dot{V}_a \rho_a c_{\mathrm{p,a}} = 1.04\,\mathrm{kJ/kg \cdot K} \tag{5.1}$$

$$\begin{aligned} q_{\max} &= C_{\min}(T_{\mathrm{w,\ in}} - T_{\mathrm{a,in}}) \\ &= 43.5\,\mathrm{kW},\ \text{per HX} \end{aligned} \tag{5.2}$$

$$\eta = \frac{q}{q_{\max}} = 0.64\,. \tag{5.3}$$

5.1.2 Winter Charging Analysis

A pseudo-transient analysis of the winter charging operation was used with the Boston weather file to find the number of units, N, needed to provide winter charging. The water temperature, $T_{\text{w, in}}$, is assumed to be representative of the average soil temperature. Initially, this is equal to the deep soil temperature, which is typically the same as the average annual outdoor air temperature, 10.6 °C. The units begin operating on November 1st and are used whenever the outside air temperature is colder than the water temperature.

The heat rejection, q, achieved every hour is calculated based on the previously calculated C_{min}, water temperature ($T_{\text{w, in}}$), and air temperature ($T_{\text{a, in}}$). The overall heat rejection energy of that hour, Q, is then distributed among the entire soil block mass to determine the water temperature for the following hour. Iterating through each hour of the weather file, starting on November 1st, q and the subsequent $T_{\text{w, in}}$ is calculated until the water temperature is found to be less than 0.1 °C. At this point, the soil block is assumed sufficiently charged.

$$T_{\text{w, in}}(\text{hour 1}) = \text{Average annual outside air temperature} \tag{5.4}$$

$$T_{\text{a, in}}(\text{hour 1}) = \text{Outside air temperature at hour 1} \tag{5.5}$$

$$q = \eta C_{\text{min}}(T_{\text{w, in}} - T_{\text{a, in}}) \tag{5.6}$$

$$Q = Nq \cdot 3600\,\text{s/h} \tag{5.7}$$

$$T_{\text{w, in}}(\text{hour 2}) = T_{\text{w, in}}(\text{hour 1}) - \frac{Q}{m_s c_{\text{v,s}}} \tag{5.8}$$

Using this analysis, $N = 11$ was found to be the minimum number of units needed to charge the soil block. In Chapter 4, the winter modeling showed that the soil block needed 55 days, or 1320 hours, for charging if supplied consistently with 0 °C water. In contrast, the HX analysis showed that the units would need to run for 2077 hours to charge the soil block. This increase was expected, as the water supplied in this method was sometimes warmer than 0 °C. After these 2077 hours, there is still an additional 174 hours remaining in the weather file when the outside air temperature is less than 0 °C to produce more cold water if needed. Any future detailed analysis of the winter modeling should incorporate the HX

analysis method into the current winter modeling algorithm to determine the hourly entering water temperature for the pipe block. However, for this level of detail, the charging time calculated is less than the 3-month charging period estimated, so the HX winter charging analysis results agree with the feasibility conclusion of Chapter 4.

5.1.3 Energy Use

The main potential drawback of using HX units as the cooling source component is its impact on the overall energy performance of the proposed system. The energy used by these 11 units was estimated based on the pressure drops given for the rated water and air flow rates (see Table 5.1) to evaluate its impact on the system performance.

$$\begin{aligned} w_{\text{pump}} &= \dot{V}_w \Delta P_w \\ &= 5.13\,\text{W} \quad \text{per HX} \\ &= 56.4\,\text{W total} \end{aligned} \tag{5.9}$$

$$\begin{aligned} W_{\text{pump}} &= w_{\text{pump}} \cdot 2077\,\text{h} \cdot 3600\,\text{s/h} \\ &= 422\,\text{MJ} \end{aligned} \tag{5.10}$$

$$\begin{aligned} w_{\text{fan}} &= \dot{V}_a \Delta P_a \\ &= 46.5\,\text{W} \quad \text{per HX} \\ &= 512\,\text{W total} \end{aligned} \tag{5.11}$$

$$\begin{aligned} W_{\text{fan}} &= w_{\text{fan}} \cdot 2077\,\text{h} \cdot 3600\,\text{s/h} \\ &= 3.83\,\text{GJ} \end{aligned} \tag{5.12}$$

Table 5.2: Heat exchanger energy use summary

Total HX energy demand	568 W
Total HX energy consumption	4.25 GJ

The energy use of the heat exchangers is summarized in Table 5.2. The energy demand of

the heat exchangers is less than 1% of the peak building latent load. The energy consumption is approximately 1.3% of the annual latent cooling load.

5.1.4 Preheat Potential

The air passing through the heat exchangers absorbs heat from the water. Since the air is warmer, it would require less work to heat that air to a comfortable indoor air temperature. Thus, if the preheated air from the HX units is used for ventilation, the heating energy use of the building could be reduced.

Assuming an indoor heating mode setpoint temperature of 18 °C, the heating load is calculated as

$$q_h = \dot{m}_{\text{ventilation}} c_{p,a} (18\,^{\circ}\text{C} - T_{\text{OA}})\,. \tag{5.13}$$

The 11 units draw a combined 9.34 m^3/s of outdoor air, which is about 25% of the maximum ventilation air requirement of the building. This limits the preheat potential of the units to less than 25% of the hourly heating load, unless the airflow through the units is increased. The cold hours when the HX units are likely to be running are not always coincident to the hours when the building is occupied. If only considering the hours when the units are running and there is a heating load present, the maximum preheat energy provided by the HX units is 1.4 kW, which is about 8% of the heating load that hour.

Overall, the total preheat provided during those coincident hours is 19 GJ, which is 0.6% of the total heating energy consumption. Although the HX units can be used to provide heating energy savings, the savings are not large enough to warrant the additional ducting needed to connect the units to the ventilation system.

5.2 Near-Surface Source Loop

The zoning requirements for the Volpe development states that at least 2 acres (8094 m^2) of the total site area must be allocated to open space (Cambridge, 2017). By placing a set of pipes near the surface of this land uncovered by buildings, the water used to charge the soil

block could be cooled by the winter air temperature permeating the shallower soil depth. This would allow the entire cooling system to only need pumping energy to move the water through all the pipes. As pumps typically require only a small percentage of building energy use, the system energy use would likely be smaller than that of typical chillers.

5.2.1 Thermal Circuit Analysis

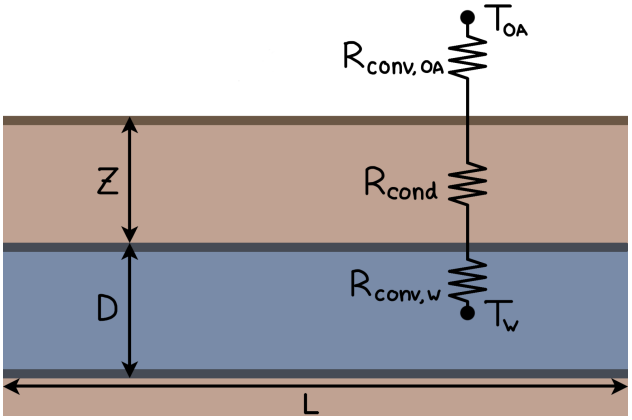

Figure 5-1: Diagram of thermal circuit for the heat transfer between outdoor air and source loop water

The performance of a near-surface loop was evaluated as a steady-state thermal circuit between the outdoor air and the water in the pipes, depicted in Figure 5-1. This calculation is intended as a rough estimate of the of the potential of the source loop, so environmental factors such as wind, snow, vegetation, solar gains, and shading, have not been included even though they can have a significant impact on the heat transferred. The total resistance of this circuit, R_{total}, is the sum of the free convection resistance between the outdoor air and the ground surface, $R_{\text{conv, OA}}$, the conduction resistance of the soil between the ground surface and the pipe, R_{cond}, and the forced convection resistance between the pipe and the moving water, $R_{\text{conv, w}}$. $R_{\text{conv, OA}}$ cannot be controlled by the loop design and $R_{\text{conv, w}}$ is not anticipated to make up a significant proportion of R_{total}. Therefore, R_{cond} is the main

variable for determining if the near-surface soil loop is possible.

$$\bar{q} = \frac{T_w - T_{\mathrm{OA}}}{R_{\mathrm{total}}} \tag{5.14}$$

$$R_{\mathrm{total}} = R_{\mathrm{conv,\ OA}} + R_{\mathrm{cond}} + R_{\mathrm{conv,\ w}} \tag{5.15}$$

The average heat transfer capacity, $\bar{q}$, required for charging the soil block was found from the building latent consumption and the number of hours when the outside air was sufficiently cold. Using this value, the maximum R_{total} allowed for the source loop is calculated, which in turn gives the maximum possible value of R_{cond}.

Annual building latent cooling consumption: 332 GJ

Number of hours outside air temperature $< 0\,^{\circ}\mathrm{C}$: 1252 h

$$\bar{q} = \frac{332\,\mathrm{GJ}}{1252\,\mathrm{h} \cdot 3600\,\mathrm{s/h}} = 73.6\,\mathrm{kW} \tag{5.16}$$

For simplicity, only one pipe was evaluated and it was assumed to have the same dimensions as the storage loop pipe block: 40 m long, 2 m pipe-to-pipe spacing, and 0.17 m pipe diameter. 101 of these pipe blocks can be fit within the 8094 m^2 of open space available. Distributing $\bar{q}$ among the 101 source loop pipes on the site means that each pipe would need to provide 729 W of cooling to charge the soil block. The average subzero outdoor air temperature used for T_{OA} is $-4.8\,^{\circ}\mathrm{C}$. Assuming that the water has reached its minimum temperature of $0\,^{\circ}\mathrm{C}$ gives the worst-case scenario for T_w. Using these two temperature values gives a conservative estimate for the temperature difference seen by the pipes.

$$R_{\mathrm{total,\ max}} = \frac{T_w - T_{\mathrm{OA}}}{\bar{q}} = 6.6 \times 10^{-3}\,\mathrm{K/W} \tag{5.17}$$

As the soil surface is warmer than the outdoor air, $R_{\mathrm{conv,\ OA}}$ can be calculated using an average Nusselt number correlation for buoyancy driven flows over the upper surface of a heated plate. The average sub-zero air temperature from the Boston weather file was used for T_∞ and the soil surface temperature, T_s, was assumed to be $5\,^{\circ}\mathrm{C}$ warmer. The exposed

soil area associated with a single pipe is $80\,\mathrm{m}^2$.

$$L_c = \frac{A}{P} = 0.95\,\mathrm{m} \tag{5.18}$$

$$\mathrm{Ra} = \frac{g\beta(T_s - T_\infty)L_c^3}{\nu\alpha} \approx 8 \times 10^8 \tag{5.19}$$

$$\overline{\mathrm{Nu}} = 0.15\mathrm{Ra}^{1/3} \approx 140 \tag{5.20}$$

$$h = \frac{\overline{\mathrm{Nu}}L_c}{k_a} \approx 3.4\,\mathrm{W/m^2K} \tag{5.21}$$

$$\begin{aligned} R_{\mathrm{conv,\ OA}} &= \frac{1}{hA} \\ &\approx 3.7 \times 10^{-3}\,\mathrm{K/W} \end{aligned} \tag{5.22}$$

A flow rate of $1\,\mathrm{kg/s}$ per pipe was chosen to provide a turbulent flow for a low $R_{\mathrm{conv,\ w}}$. The Nusselt number was calculated using the following Gnielinski Nusselt number correlation (Incropera and DeWitt, 2002)

$$f = (0.79\ln \mathrm{Re}_D - 1.64)^{-2} \tag{5.23}$$

$$\mathrm{Nu}_D = \frac{(f/8)(\mathrm{Re}_D - 1000)\mathrm{Pr}}{1 + 12.7(f/8)^{1/2}(\mathrm{Pr}^{2/3} - 1)} \tag{5.24}$$

that was appropriate for the range of Reynolds numbers achieved by the flowrates. As expected, $R_{\mathrm{conv,\ w}}$ has little impact on R_{total} in comparison to $R_{\mathrm{conv,\ OA}}$, as it is 2 orders of magnitude smaller. Therefore, increasing the flow rate to further reduce the resistance in the pipe would only increase pump energy without affecting R_{total}.

$$u = \frac{\dot{m}_w}{\rho_w \pi {D_p}^2/4} = 0.04\,\mathrm{m/s} \tag{5.25}$$

$$\mathrm{Re}_D = \frac{\rho_w u D_p}{\mu} = 4280 \tag{5.26}$$

$$f = (0.79 \ln Re_D - 1.64)^{-2} \tag{5.27}$$

$$\mathrm{Nu}_D = \frac{(f/8)(\mathrm{Re}_D - 1000)\mathrm{Pr}}{1 + 12.7(f/8)^{1/2}(\mathrm{Pr}^{2/3} - 1)} = 157 \tag{5.28}$$

$$\begin{aligned} R_{\mathrm{conv,\ w}} &= \frac{1}{hA} = \frac{D_p}{\mathrm{Nu}_D\, k_w (\pi D_p L)} \\ &\approx 8 \times 10^{-5}\,\mathrm{K/W} \end{aligned} \tag{5.29}$$

Having calculated R_{total}, $R_{\mathrm{conv,\ OA}}$, and $R_{\mathrm{conv,\ w}}$, the maximum possible value of R_{cond} can be found. Assuming that the 2 m spacing between pipes is sufficiently large such that there is negligible effect from the adjacent pipes, the shape factor method for a pipe buried in a semi-infinite medium can be applied to calculate R_{cond} (Incropera and DeWitt, 2002). The shape factor, S, is determined by the geometry of the pipe and the depth at which it is buried under the surface. As the pipe geometry has already been set, the value of S that satisfies the conditions on R_{cond} and R_{total} will give the minimum pipe burial depth, z.

$$R_{\mathrm{cond}} = R_{\mathrm{total}} - R_{\mathrm{conv,\ OA}} - R_{\mathrm{conv,\ w}} = 2.8 \times 10^{-3}\,\mathrm{K/W} \tag{5.30}$$

$$R_{\mathrm{cond}} = \frac{1}{S k_w} \tag{5.31}$$

$$\frac{1}{R_{\mathrm{cond}} k} = S = \frac{2\pi L}{\cosh^{-1}(2z/D_p)} \tag{5.32}$$

$$\begin{aligned} z &= \frac{D_p}{2} \cosh\left(2\pi L R_{\mathrm{cond}} k_w\right) \\ &= 0.24\,\mathrm{m} \end{aligned} \tag{5.33}$$

5.2.2 Pump Energy Estimate

The minimum pipe depth is quite shallow, so it is not feasible to reduce the number of pipes in the source loop and the source loop will need to cover the entire 2 acres of open space allocated in the zoning text. If all 101 source loop pipes are assumed to be in one continuous straight length, the pressure drop due to friction losses, ΔP_f, can calculated using Equation 3.16. This is then used with Equation 3.21 to estimate the pump energy, w_f, needed to overcome this pressure drop.

$$L = 101 \cdot 40\,\text{m} = 4.04\,\text{km} \tag{5.34}$$

$$f = 0.04 \tag{5.35}$$

$$\Delta P_f = 891\,\text{Pa} \tag{5.36}$$

$$w_f = 101\frac{\dot{m}_w}{\rho_w}\Delta P_f = 90\,\text{W} \tag{5.37}$$

$$W_f = w_f \cdot 1252\,\text{h} \cdot 3600\,\text{s/h} = 406\,\text{MJ} \tag{5.38}$$

The value of w_f calculated is a low estimate for the overall pump energy of the source loop. As the open space is unlikely to be one continuous area, the source loop pipes may be spread far from the building. Therefore, the total pipe length for the source loop would be longer than 4 km, increasing the friction losses. The pipes would not fit on the site at one continuous straight path, so tees and bends would also be needed for a realistic piping network. The pressure losses due to these fittings can be larger than the pressure losses due to friction, so the overall pump energy with fittings included could be significantly higher than w_f.

5.3 Comparison

The near-surface source loop was proposed to minimize the energy use of the system by taking advantage of the VolpeMIT zoning requirements and eliminating fan energy use. The pump energy associated with friction losses, W_f, for the near-surface source loop is approximately equal to the HX pump energy and is about 10% of the total HX energy use. Although the

scale of the near-surface source loop makes it difficult to derive a reasonable estimate for its total pump energy usage, this rough estimate confirms that a pumping only system uses less energy than a system with fans.

However, the scale of the piping loop needed to achieve the required heat transfer rate is impractical. First, these pipes must be buried at a very shallow depth. This could result in less attractive open spaces as vegetation and playground equipment would have to be chosen so as not to disturb the pipes below. Furthermore, the source loop needs to cover a large area, roughly 5 times the building footprint in this case. This is generally not feasible in dense cities and is only possible at the VolpeMIT site if all the open space available in this multi-building development is used to serve just one building. Furthermore, the near-surface source loop requires at least 4 km of piping and the excavation of an 8094 m^2 area, so its installation cost is likely to be high.

In contrast, the HX units can be installed on the building roof without taking up any valuable floorspace in the building or on the site. As this is a readily-available commercial option, the equipment and installation costs are likely to be competitively priced and building managers are probably already familiar with the maintenance of the units.

The heat exchangers offer some flexibility in their operation which increases the likelihood of successful winter charging. If the winter is mild, reducing the ΔT between the water and outside air, the units could be run at a higher air flow rate to maintain the heat transfer needed, at the cost of increased fan energy use. Increasing the water flow rate in the source loop does not produce a similar effect as the convection resistance of water was shown to have minimal impact on the source loop total thermal resistance. As previously mentioned, the near-surface source loop was also calculated without including the impact of environmental factors such as snow or shading, which could further reduce its charging potential. Therefore, the heat exchangers are more resilient to changing weather conditions.

In conclusion, heat exchangers should be used as the cooling source to charge the soil block in winter. The fan energy they use increases the overall energy use of the proposed system but this is an acceptably small penalty as they are far more feasible to install and operate than a near-surface soil block.

Chapter 6

Summer Modeling

Since the winter modeling showed that the soil block could be charged within the 3-month winter season, the proposed system has a source of cooling to produce low temperature water for dehumidification in summer. However, summer modeling is needed to test if this low temperature water can be provided consistently throughout the season. The summer modeling also tests the ability of the system to react to fluctuations in the latent loads.

The model geometry used for the summer modeling is the same as that used in the winter model, with the pipe block modeled as nine 2-D slices. The pipe spacing $D_s = 2\,\text{m}$ model is used as the results in Section 4.6.1 showed that there was not a sufficiently large difference in temperatures to necessitate using the effective soil diameter model to include the corner soil.

The summer modeling follows the process described in the Figure 6-1 flowchart. The code calls the subroutine described by Figure 6-3 to model each day in the latent cooling period. Both processes call the entering water temperature calculation function described in Figure 6-2. These flowcharts provide an overview of the summer modeling method and the details of the steps involved are described throughout this chapter.

6.1 Initial and Boundary Conditions

The soil block starts at a uniform temperature of $0\,^{\circ}\text{C}$ based on the results showing that the winter charging period was successful. The soil block is also assumed to see adiabatic

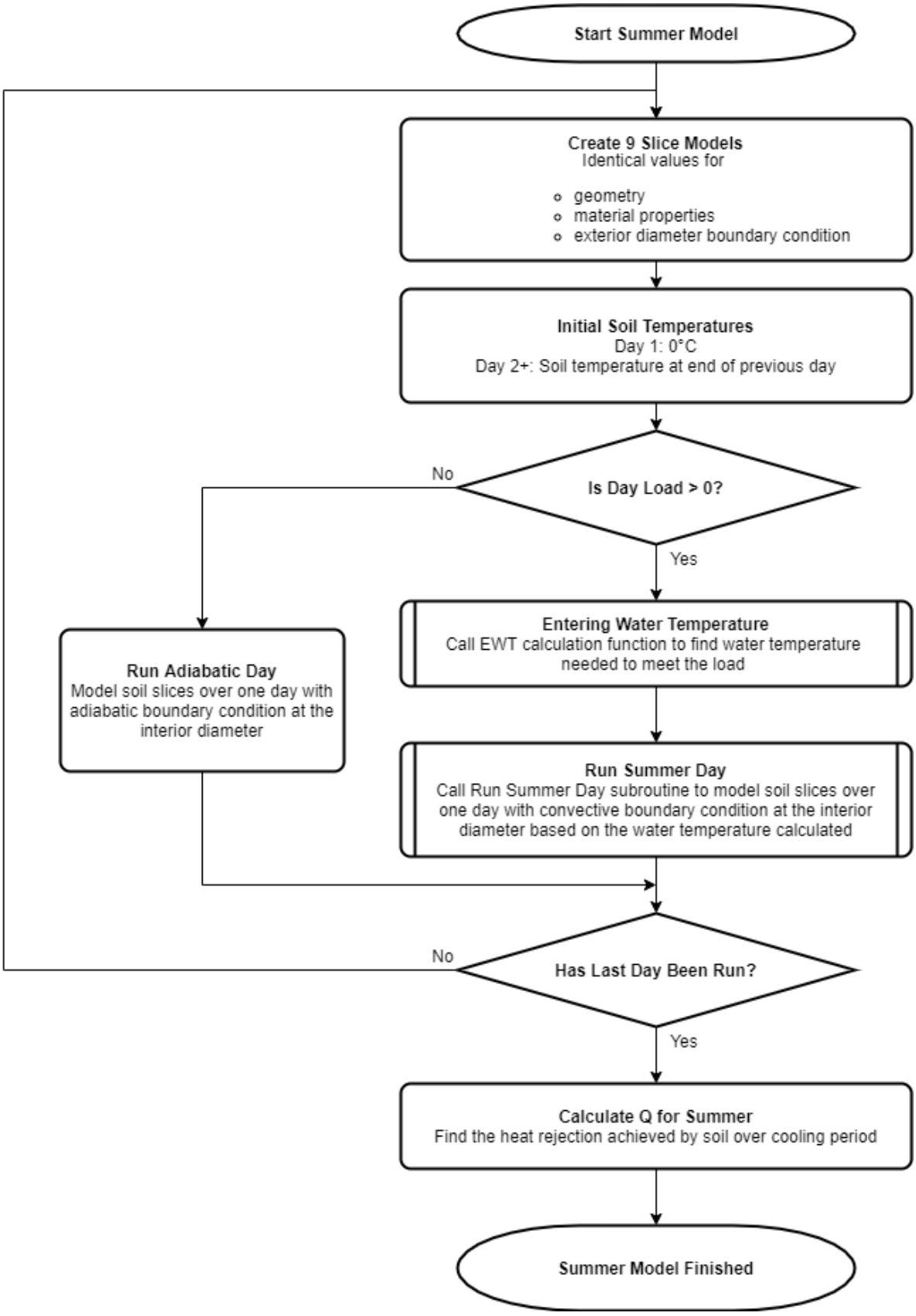

Figure 6-1: Flowchart of summer modeling process

conditions between seasons, such that any temperature gradients within the soil are further diminished.

As in the winter modeling, the soil at the outer diameter of the slice model, D_s, sees an adiabatic boundary condition due to symmetry with the adjacent pipe blocks. The pipe edge of the slice, D_p, sees a convective boundary condition with a varying ambient temperature from the water flow through the pipe. The convective resistance, h, is dependent on the mass flow and the geometry of the pipe and is constant along the pipe. The ambient, or bulk water, temperature is the average Entering Water Temperature (EWT), T_w, for each slice, which is dependent on the heat transfer through the previous slice. The EWT calculation is described in further detail in Section 6.3.

The MATLAB PDE toolbox solves Equation 4.4 with a timestep of 200s for the nodal temperatures of the slice. Equations 6.1 and 6.2 are applied as boundary conditions at the pipe and soil boundaries respectively, highlighted in Figure 4-4. As described in Chapter 4, the axial temperature gradients in the soil between slices are neglected. The initial condition is given by Equation 6.3.

$$\frac{\partial T(r_p,t)}{\partial r} = \begin{cases} h(T(r_p,t) - T_w(t)), & \text{if equipment is on and latent load} > 0 \\ 0, & \text{otherwise} \end{cases} \tag{6.1}$$

$$\frac{dT(r_s,t)}{dr} = 0 \tag{6.2}$$

$$T(r, t=0) = 0 \tag{6.3}$$

6.2 Building Loads

The system tries to meet the latent loads calculated in Chapter 2. The hourly loads are aggregated into daily totals and then divided by the 16 hours when the equipment is on, giving daily average loads. Using daily loads rather than averaging the annual load over the summer months allows the simulation to test how the system handles load peaks. Running the system for 16 hours and shutting it off for 8 hours reflects the anticipated building HVAC schedule and allows the model to include the effect of the soil temperature gradient settling

overnight. It is possible to simulate meeting the loads on an hourly basis, instead of using the daily averages, but this was considered excessively detailed for a feasibility study.

The loads are divided by the number of pipes in the soil block. This implies that all pipes will be simultaneously active throughout the season. An initial attempt was made to stage the pipes such that a small number of pipes were used for the low early summer loads and additional pipes were only made active when the previous pipes could no longer handle the loads. However, designing these staging controls proved to be more difficult than anticipated, and so it was put aside for future work. Therefore, the load that each pipe block tries to meet each day is

$$q_{\text{load}} = \frac{\text{Average building latent cooling demand when equipment is on}}{\text{number of pipes}}. \tag{6.4}$$

The summer model starts and ends with the first and last day that have latent cooling loads. This period extends all the way into November, overlapping with the time when we might expect to start charging the soil block. This larger than expected cooling period may be the result of the strict thermal comfort limit used in the calculation, as discussed in Chapter 2. Although there may be some potential for charging in this overlap period, the system attempts to meet the summer loads using only the cooling that was stored during the previous winter charging. Future work could potentially look into the possibility of using favorable outdoor weather conditions to recharge the soil during the summer period.

On the days when there is no daily load, the model is run with an adiabatic boundary condition at D_p to simulate the effect of time on the soil temperatures. During this time, the warmer parts of the soil will conduct heat to the cooler areas, reducing the temperature of the soil close to the pipe even though the overall average temperature remains the same. This has a noticeable impact on the heat rejection of the following day, hence the zero-load days must also be modeled.

6.3 Entering Water Temperature Calculation

The temperature of the water entering the pipe is adjusted to control the amount of heat rejected by the water as it passes through the soil block. If the heat rejected is larger than the latent load, the excess cooling is wasted in over-dehumidifying the air and diminishes the stored cooling potential of the soil block. A storage tank could be used to hold any excess cold water to be used for later loads, but it is still preferable to minimize overcooling so that a small tank would suffice. The heat rejected could also be controlled by adjusting the water mass flow rate but a sensitivity analysis showed that this method was more difficult to implement and could lead to unreasonably high flow rates. This analysis is explained in further detail in 6.6.

A separate function, shown in flowchart form in Figure 6-2, is used to iteratively calculate the appropriate Entering Water Temperature (EWT) to use in the transient simulation. This function takes in the load to be met, the soil temperatures, and an initial guess for the EWT. The load to be met, q_{limit}, is the average latent load calculated for the day when the function is called. The soil temperatures, $T_s(n)$, are the temperatures of the soil at each slice n at the time when the function is called.

Before calculating the EWT, q_{load} is increased by 15% such that

$$q_{\text{limit}} = 1.15 q_{\text{load}} \tag{6.5}$$

where q_{limit} is the inflated load that the function is trying to meet. The resultant EWT will produce some overcooling, since it is meeting a larger load, but this allows it to meet the actual q_{load} for a longer period of time than if it were calculated for q_{load}. If using the actual load, the EWT would have to be recalculated and the transient simulation rerun more often, significantly increasing the simulation time. The 15% overcooling loss is considered an acceptable loss in exchange for the simulation benefits.

Solving the energy balance for the heat loss from the water against the heat gain of the soil gives the temperature of the water leaving the soil slice. Solving this for each slice in

sequence gives the overall Leaving Water Temperature (LWT) for the pipe.

$$\dot{m}_w c_{p,w} \frac{dT_w}{dx} = -h\pi D_p L(T_w - T_s(r_p, t)) \tag{6.6}$$

$$T_{w,out} = e^{-\frac{h\pi D_p}{\dot{m}_w c_{p,w}}}(T_{w,in} - T_s(r_p, t)) + T_s(r_p, t) \tag{6.7}$$

$$T_{w,in}(\text{slice n+1}) = T_{w,out}(\text{slice n}) \tag{6.8}$$

The exponent $\frac{-h\pi D_p}{\dot{m}_w c_{p,w}}$ is flow and geometry dependent, so it is constant for all slices. $T_s(r_p, t)$ is the average soil temperature around the pipe boundary for slice n at time t. This is assumed to be constant in the length between slice n and slice n+1. Slice 1 uses T_{guess} for $T_{w,in}(1)$ and all subsequent slices use values calculated based on the preceding slice until a value is found for the LWT of the last slice.

If the heat rejection, q_w, calculated from the resultant temperature difference as

$$q_w = \dot{m}_w c_{p,w}(T_{\text{guess}} - \text{LWT}) \tag{6.9}$$

is less than q_{limit}, T_{guess} is too low. The process is repeated with higher values of T_{guess} until a value is found that produces a temperature difference that meets q_{limit}. At this point, q_w is larger than q_{limit} and T_{guess} would produce more than 15% overcooling if used as the EWT in the model. Therefore, the EWT is found through linear interpolation as

$$q_{w,\text{low}} = \dot{m}_w c_{p,w}(T_{\text{guess, low}} - \text{LWT}_{\text{low}}) < q_{\text{limit}} \tag{6.10}$$

$$q_{w,\text{high}} = \dot{m}_w c_{p,w}(T_{\text{guess, high}} - \text{LWT}_{\text{high}}) \geq q_{\text{limit}} \tag{6.11}$$

$$\text{EWT} = \frac{q_{\text{limit}} - q_{w,\text{low}}}{q_{w,\text{high}} - q_{w,\text{low}}}(T_{\text{guess, high}} - T_{\text{guess, low}}) + T_{\text{guess, low}} \tag{6.12}$$

to get a value that best meets q_{limit}.

When the function is called over the course of the day, as described in the following section, the estimated EWT value, T_{guess}, is set to the previous EWT value used because the next EWT needed is unlikely to be significantly larger. However, when called at the start of the day, T_{guess} is set to maximum temperature in the soil at that instant to account for overnight changes in soil temperature. When the equipment is turned off at the end of the day

and over the weekend, heat continues to be conducted away from the pipe boundary towards the cooler outer soil, reducing the pipe boundary temperatures, $T_s(r_p, t)$. In some cases, q_{limit} is also lower than for the previous day, so a smaller temperature difference between EWT and LWT is needed. The cooler pipe temperatures and lower q_{limit} mean that reusing the previous EWT value could cause excessive overcooling. The maximum soil temperature, is lower than the previous EWT, so it provides a more accurate guess when starting a new day and allows the EWT to fluctuate as needed to reduce overcooling.

6.4 Run Summer Day

For the days when there is a load, q_{load}, the system model tries to meet the load for the time when the equipment is on. The model is run for an 8-hour period. The ambient temperature used for the convective boundary condition of the first slice is the water temperature produced by the EWT function. After the first slice has been modeled for the 8-hour period, an energy balance for the heat gained by the soil at every time step is used to calculate the temperature of the water leaving the slice. As described for the EWT function, the temperature of the water leaving slice 1 used as the entering water temperature for slice 2, which is then modeled for the same 8-hour period. The model iterates over each of the slices until the LWT values have been found for the final slice in the pipe.

The heat rejected at each time step, $q_w(t)$ is calculated from the EWT of the first slice and the LWT of the last slice

$$q_w(t) = \dot{m}_w c_{p,w}(\text{EWT}(t) - \text{LWT}(t)) \; . \tag{6.13}$$

These values of $q_w(t)$ are compared against the q_{load} that the system is trying to meet that day. Just as 15% overcooling was considered acceptable, 15% undercooling was also considered acceptable in order to lengthen the time when the load was considered satisfied and reduce recalculation. In the example scenario shown in Figure 6-4a, $q_w(t) \geq 0.85 q_{\text{load}}$ for the entire 8-hour period, so the results for the whole period are saved.

The model then runs for the following 8-hour period, with the soil temperatures initialized

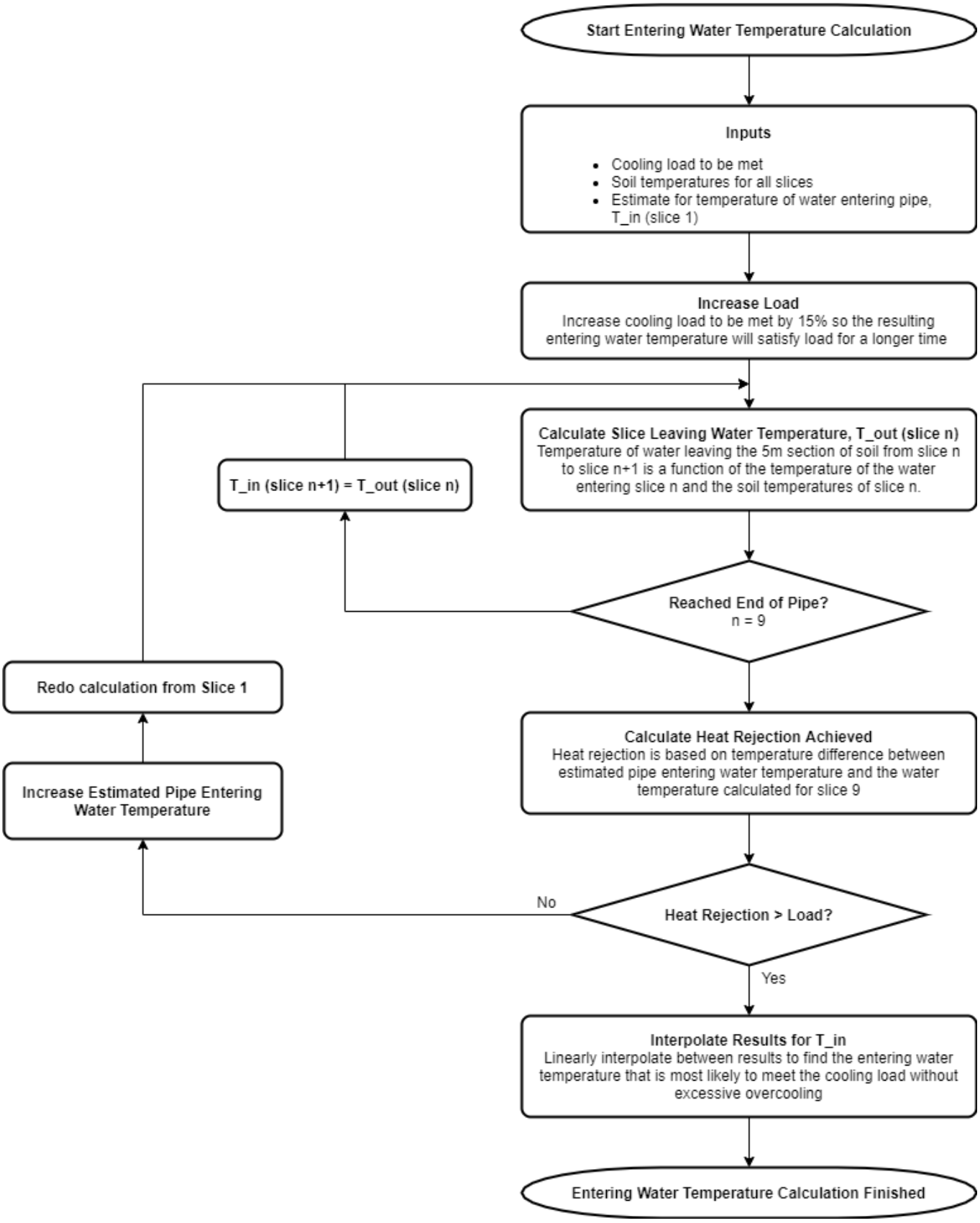

Figure 6-2: Flowchart of function for calculating pipe block entering water temperature

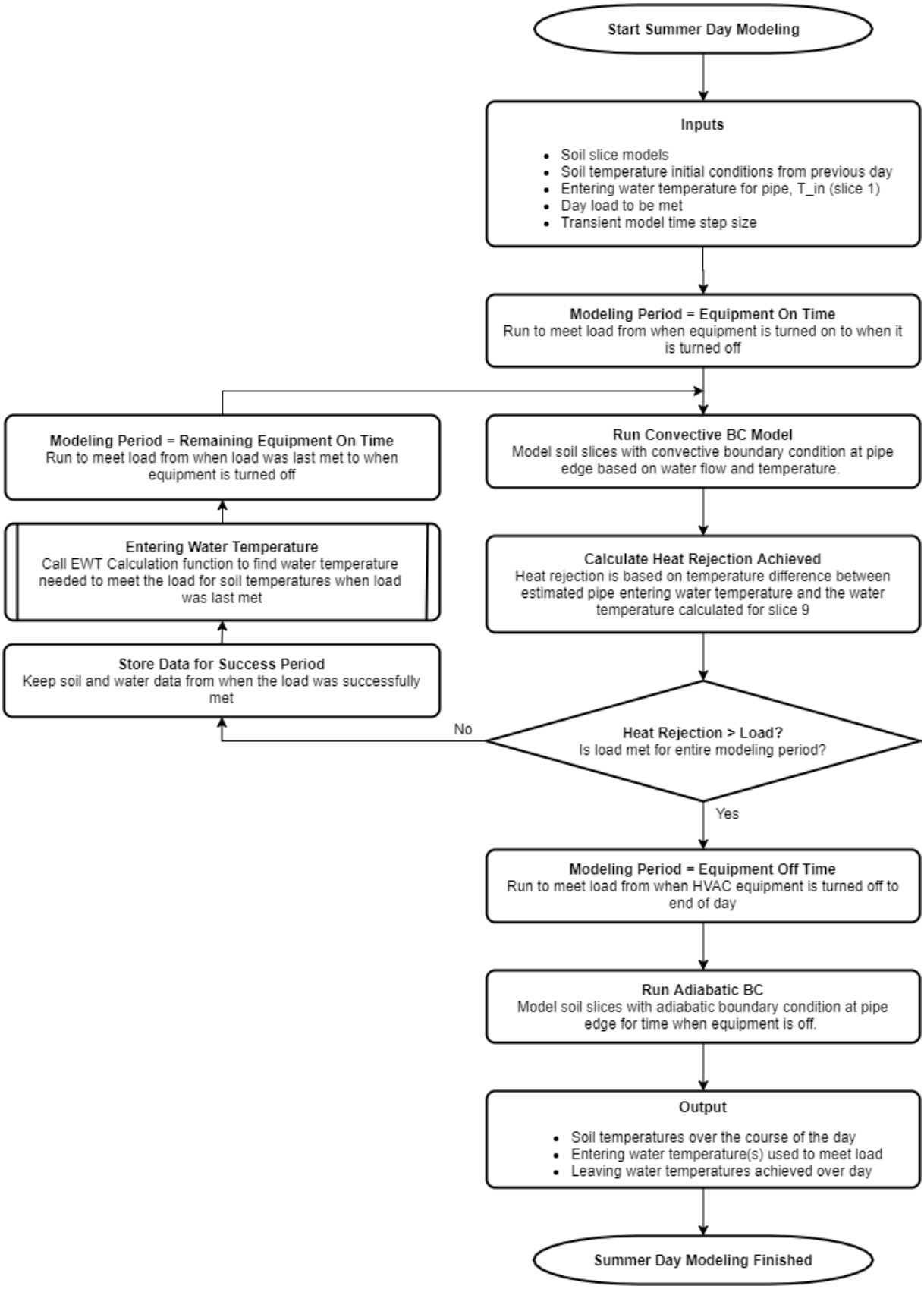

Figure 6-3: Flowchart of subroutine for modeling one day of summer cooling

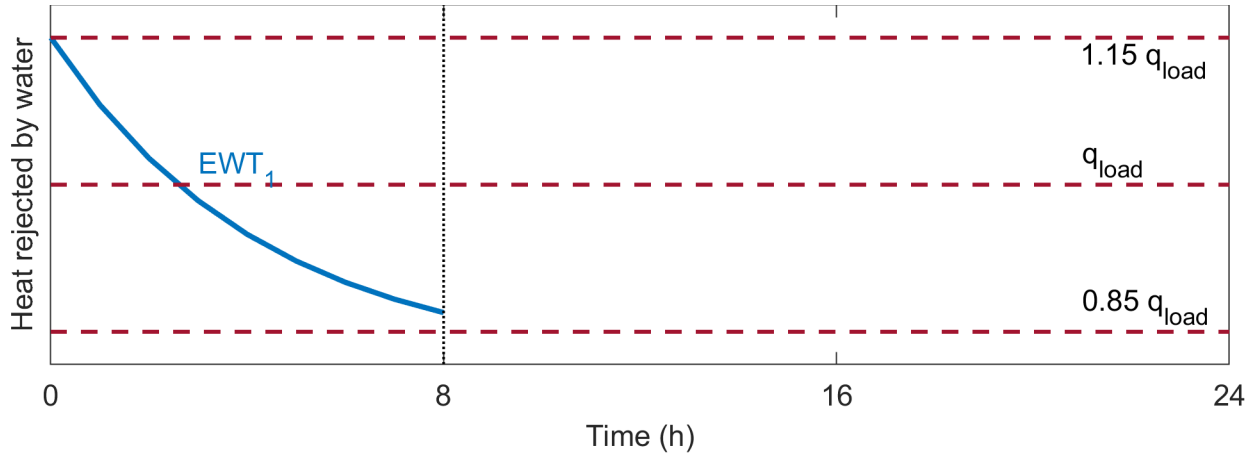

(a) Heat rejected by water meets load for whole first 8-hour period, from t = 0 to 8, using EWT_1

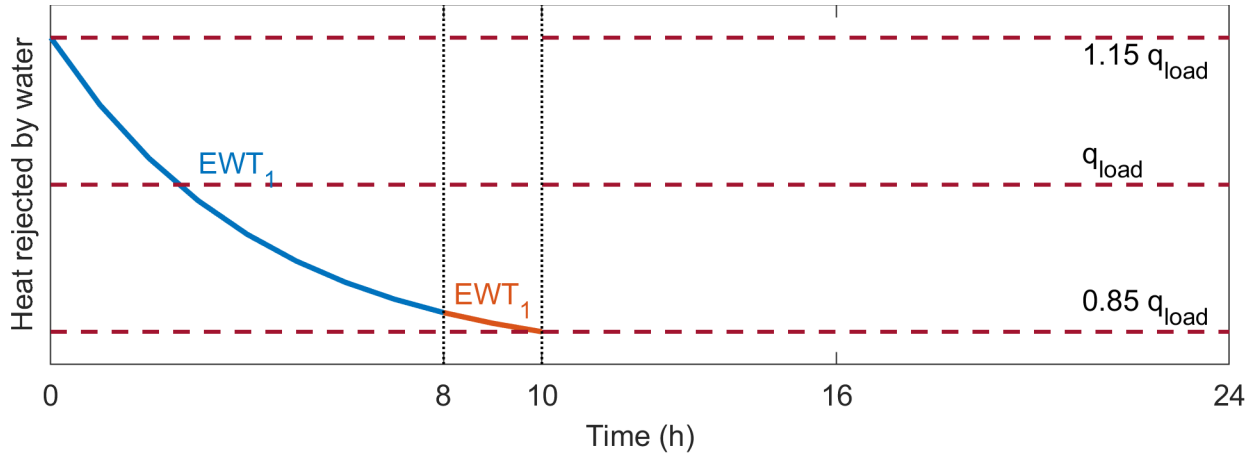

(b) Heat rejected by water meets load for part of second 8-hour period, from t = 8 to 10, using EWT_1

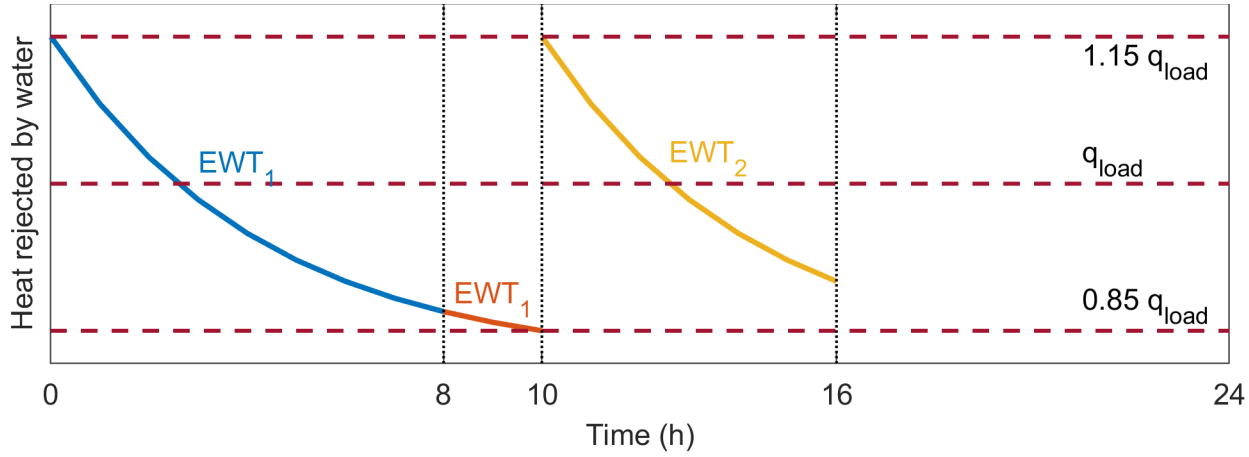

(c) Heat rejected by water meets load for remainder of day when equipment is on, from t = 10 to 16, using EWT_2

Figure 6-4: Example scenarios for entering water temperature recalculation based on heat rejection achieved in successive 8-hour modeling time periods

as the temperatures saved at $t = 8$ hours. Since the previous water temperature used, EWT_1, was still successful at the end of the time period, the second 8-hour period is also run with EWT_1. In the example shown in Figure 6-4b, using EWT_1 value produces sufficient heat rejection for 2 more hours, up to $t = 10$ hours. The results for these two hours are saved and the results for the rest of the time, $t = 10$ to 16, are discarded.

The soil temperatures from $t = 10$ hours and the EWT used are sent to the EWT function to calculate the increased water temperature, EWT_2, needed to continue to meet the load for the rest of the day. The model runs for another 8-hour period, from $t = 10$ to 18, with the soil temperatures initialized as the values from $t = 10$ hours and using EWT_2. In the example shown in Figure 6-4c, the heat rejection using EWT_2 is successful for the rest of the time when the equipment is on. The results for the last 2 hours, $t = 16$ to 18, are discarded because the equipment is no longer active during that time.

Once the load has been met for the entire day, $t = 0$ to 16, the model is run for the final 8-hour period in the day when the equipment is off, using the adiabatic pipe boundary condition case for Equation 6.1. The soil temperatures are initialized as the results from $t = 16$. The soil temperatures for the following day will be initialized as the results from $t = 24$. As described in Section 6.3, EWT_2 will not be used as the initial T_{guess} for the EWT function for the following day, since that value could produce overcooling.

For days when there is no load, the model is run for a 24-hour period using the adiabatic pipe boundary condition case for Equation 6.1. The soil temperatures are initialized as the results from $t = 24$ for the previous day. The results for all 24 hours are saved.

The summer model iterates through latent cooling period, calling the Run Summer Day procedure for each day until all loads have been met.

6.5 Summer Performance

Once all the days with latent loads have been modeled, the model of the summer operation of the system is complete. Since the model is controlled to meet the load on a daily basis, the overall summer heat rejection modeled meets the annual building latent load of 332 GJ. However, the method of control was to increase the entering water temperature without

considering the water temperatures needed for dehumidification. Previous calculations in Chapters 3 and 4 assumed that the water temperature would remain under 10 °C based on the dewpoint temperature target. However, using this somewhat arbitrary 10 °C cap severely limits the time when the summer operation is successful. Therefore, a more accurate value for the maximum dehumidifier water temperature possible must be found to see if the leaving water temperatures obtained are sufficiently cold throughout the season.

6.5.1 Dehumidifier

The dehumidifier is essentially a heat exchanger that the excess water vapor condenses on. A heat exchanger was sized to dehumidify the outside air to 0.010 kg/kg to meet the thermal comfort conditions described in Chapter 2.1.

The outside air properties were based on the average drybulb temperature and humidity ratio for the times when there is a latent load. The dehumidified supply air properties were based on the humidity ratio required and its associated dewpoint temperature. The associated enthalpies for both were found from a psychrometric chart. Based on these properties, given in Table 6.1, an equivalent average specific heat capacity, $\overline{c}_{p,a}$, could be calculated for the air passing through the heat exchanger. The heat capacity rate for the air-side of the heat exchanger, C_H, is calculated from this average specific heat capacity and the ventilation air flow rate.

Table 6.1: Outside air and supply air psychrometric properties

	Outside Air (OA)	Supply Air (SA)
Humidity ratio, ω (g/kg)	18	10
Enthalpy, h, (kJ/kg)	67.7	39.8
Dry-bulb temperature, T (°C)	22.8	14.4

$$\Delta h = \overline{c}_p \Delta T \tag{6.14}$$

$$\overline{c}_{p,a} = \frac{h_1 - h_2}{T_{OA} - T_{SA}} = 3.3\,\text{kJ/kg} \cdot \text{K} \tag{6.15}$$

$$\dot{m}_{air} = \text{Ventilation rate} = 45.8\,\text{kg/s} \tag{6.16}$$

$$C_H = \dot{m}_a * \bar{c}_{p,a} = 152\,\text{kW/K} \tag{6.17}$$

The water-side heat capacity rate for the heat exchanger is calculated based on the total water flow rate of all the pipes. The heat exchanger was assumed to have an NTU value of 3. Based on the NTU-epsilon relations for a single pass, cross-flow heat exchanger, the effectiveness of the heat exchanger is found to be $\epsilon = 0.8$ (Incropera and DeWitt, 2002).

$$\dot{m}_w = 1\,\text{kg/s} \cdot \text{pipe} * 80\text{pipes} = 80\,\text{kg/s} \tag{6.18}$$

$$C_C = \dot{m}_w * c_{p,w} = 80\,\text{kg/s} * 4.2\,\text{kJ/kg} \cdot \text{K} = 336\,\text{kW/K} \tag{6.19}$$

$C_C > C_H$, therefore, $C_{max} = C_C$ and $C_{min} = C_H$ and

$$C_{max}/C_{min} = 2.21\,. \tag{6.20}$$

$$\epsilon = \frac{Q}{Q_{max}} = \frac{C_H \Delta T_H}{C_{min}(T_{H,in} - T_{C,in})} \tag{6.21}$$

$$T_{H,in} - T_{C,in} = \frac{\Delta T_H}{\epsilon} \tag{6.22}$$

$$\begin{aligned} T_{C,in} &= T_{H,in} - \frac{\Delta T_H}{\epsilon} \\ &= T_{OA} - \frac{T_{OA} - T_{SA}}{\epsilon} \\ &= 12.3\,^\circ\text{C} \end{aligned} \tag{6.23}$$

Based on the air-side conditions given, the water temperature provided to the dehumidifier must be less than or equal to 12 °C to sufficiently dry the incoming air. If the water temperature is higher than this, the desired dehumidification could still be achieved by increasing the flow rate of the water through the dehumidifier, although this will have diminishing effect. Once the water reaches the drybulb temperature of 14 °C, the dehumidifier can no longer produce sufficiently dry air, regardless of flow rate.

6.5.2 Results

With the load distributed among 80 pipes in the soil block, the resultant LWT shown in Figure 6-5 remain below this threshold until August. After this point, the water temperature fluctuates between the acceptable and unacceptable ranges. This fluctuation is the result of the evening adiabatic 'rest', which allows the heat in the area close to the pipe to diffuse through the rest of the soil, lowering the temperature in the near-pipe area. This improves the heat transfer potential for the following day. When there are several consecutive high load days, the overnight period does not offer sufficient heat diffusion, resulting in excessively high LWT for the following day.

Before the final latent load in November, the system is not used for a long period of time but the resultant LWT is still above the dehumidifier limit of 12 °C. This is not due to the temperature gradients within the soil, as that has had time to even out. Instead, it implies that the heat rejection potential of the system is no longer sufficient at this point.

As a test case, the model was run with the load distributed among 100 pipes, such that the pipe block modeled is meeting 1% of the building latent load. The results for this simulation are shown in Figure 6-6. In this case, the LWT is never higher than the dewpoint temperature and is only higher than the dehumidifier temperature for 2 days. In this case, the final LWT is lower than the dehumidifier limit, so it has not exhausted its cooling potential. Adding 20 pipes to the system design would increase the soil block height from 8 m to 10 m and would generally increase the pump energy use and installation costs, so simply adding pipe blocks to the designed soil block is not the most practical means of improving the system. Nonetheless, these results indicate that the system sizing process may need further refinement to consistently produce sufficiently cold water throughout the season.

It is possible that the 80 pipes might be able to meet the temperature requirements if the omitted corner soil was included in the pipe block model, thereby increasing the volume of soil available for the heat to be diffused into. Alternatively, the soil block sizing may have been insufficient to meet the cumulative impact of the 15% load oversizing described in Section 6.3. In this case, the overall soil block would need to be oversized accordingly or

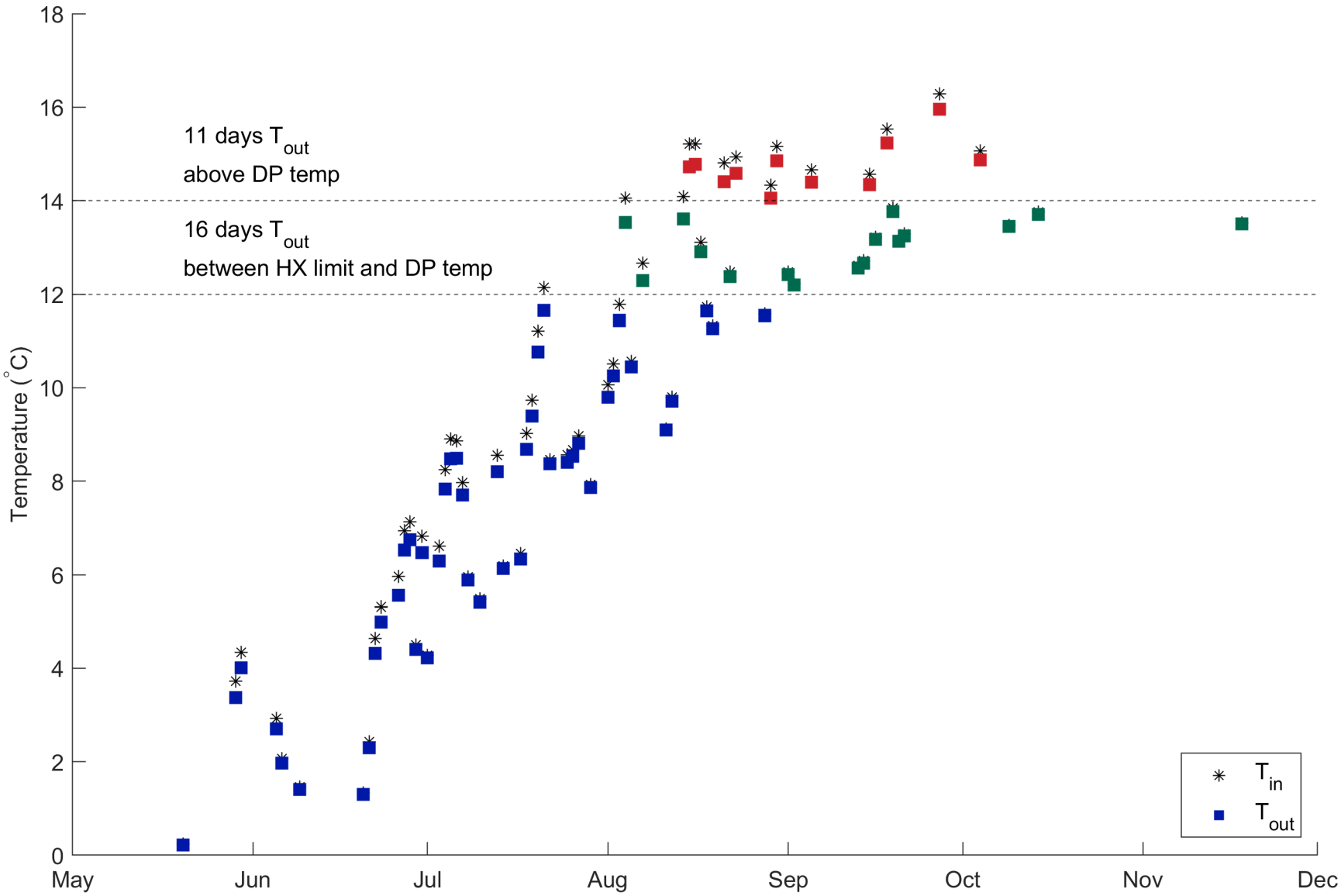

Figure 6-5: Entering and leaving water temperatures for 80 pipes

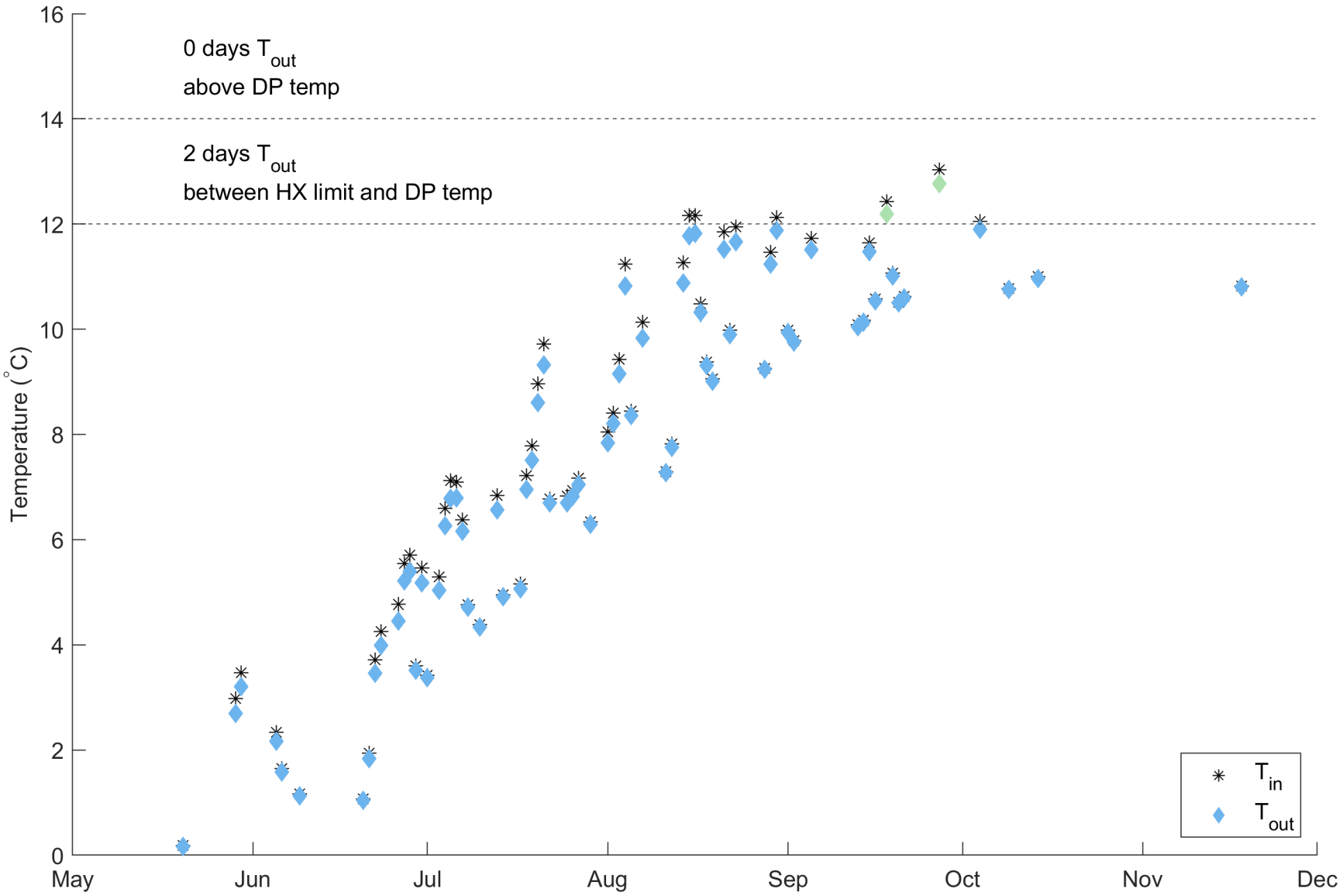

Figure 6-6: Entering and leaving water temperatures for 100 pipes

the 15% oversizing method might need to be reduced.

If the pipe blocks were staged instead of using them all simultaneously, it might be possible to keep the LWT below the dehumidifier limit for longer. For example, if only 10 pipes were used initially, the water produced would eventually approach 12 °C. However, at that point, a second set of 10 pipes, all still at the initial temperature of 0 °C, would be used to further decrease the water temperature away from the limit. This could prevent the water temperature from climbing too rapidly when there are consecutive high load days.

Overall, the summer modeling results show that the proposed system can use the cooling stored in the charged soil block to produce cold water for dehumidification throughout the summer period. The system is also able to respond to fluctuations in the latent load demand by using the EWT control method. However, further refinement of soil block sizing and pipe block staging is needed for the system to consistently provide sufficiently cold water throughout the cooling period.

6.6 Control Method Sensitivity Analysis

At first glance, $q = \dot{m}_w c_{p,w}(T_{w,in} - T_{w,out})$ seems to imply that the heat rejected by the water is directly proportional to the mass flow and EWT, making them equally useful control variable options. However, Equation 6.7 shows that LWT is also a function of mass flow and EWT. Aside from the terms appearing explicitly in the equation, the convective heat transfer coefficient, h, is also dependent on mass flow. Increasing the mass flow increases h such that the net effect on the exponent term is unclear. Therefore, the impact of mass flow and EWT on the heat rejected by the water is not as straightforward as initially assumed.

To compare the impact of the two variables, heat rejection was calculated for mass flows ranging from 0.5 kg/s to 5 kg/s and EWT from 0.5 °C to 5 °C. The water was considered to be passing through one soil slice, 5 m travelled, such that it sees a constant soil temperature throughout, since axial temperature variation is neglected between slices. Equations 5.23 and 5.24 are used to find the heat transfer coefficient associated with the water flow.

The LWT was calculated for all combinations of mass flow and EWT values. The temperature differences, $\Delta T = EWT - LWT$, and heat rejection values, $q_w = \dot{m}_w c_{p,w} \Delta T$, were

then found for all EWT and mass flow combinations.

The resultant data, shown in Figure 6-7, shows the impact of the control variables as comparable. In the figure, if a line is labeled as having a constant EWT, then the x-axis is showing increasing mass flow, and vice versa for the constant m labels. Although the cases shown result in relatively similar heat rejection trends, the chart implies that holding the EWT constant and increasing the mass flow would provide greater heat rejection, thereby making it the better control variable.

Nonetheless, the soil temperature will inevitably increase as it absorbs heat from the water, thereby reducing the heat rejection achieved with either strategy. The soil temperature was increased from 0 °C to 0.3 °C and the heat rejection was recalculated each time. The results shown in Figure 6-8 show that the relative impact of the increased mass flow decreases as the soil warms up. Although the heat rejection achieved for the EWT control strategy also decreases, the relative impact of each EWT increase is unchanged. Therefore, the mass flow control strategy would require the mass flow to be increased by larger increments over time to counteract the impact of the warmer soil while the EWT control strategy can use smaller increments to achieve the same effect.

Taking the soil temperature increase into account shows that mass flow control is not adequate for meeting summer cooling loads. As the soil warms up over time, the mass flow required could grow excessively, increasing the pump energy used by the system and negating the efficiency benefits of the proposed system. In contrast, keeping the mass flow constant and controlling EWT is unlikely to have a significant impact on the pump energy used. the increased EWT would probably be produced by mixing warmer and colder water streams to get the desired temperature and the mixing valves needed for this would have a smaller impact on pump energy than increasing the mass flow tenfold. Thus, the sensitivity analysis of these two control variables concludes that the EWT control strategy is the more effective and practical method of controlling the heat rejection in the soil block.

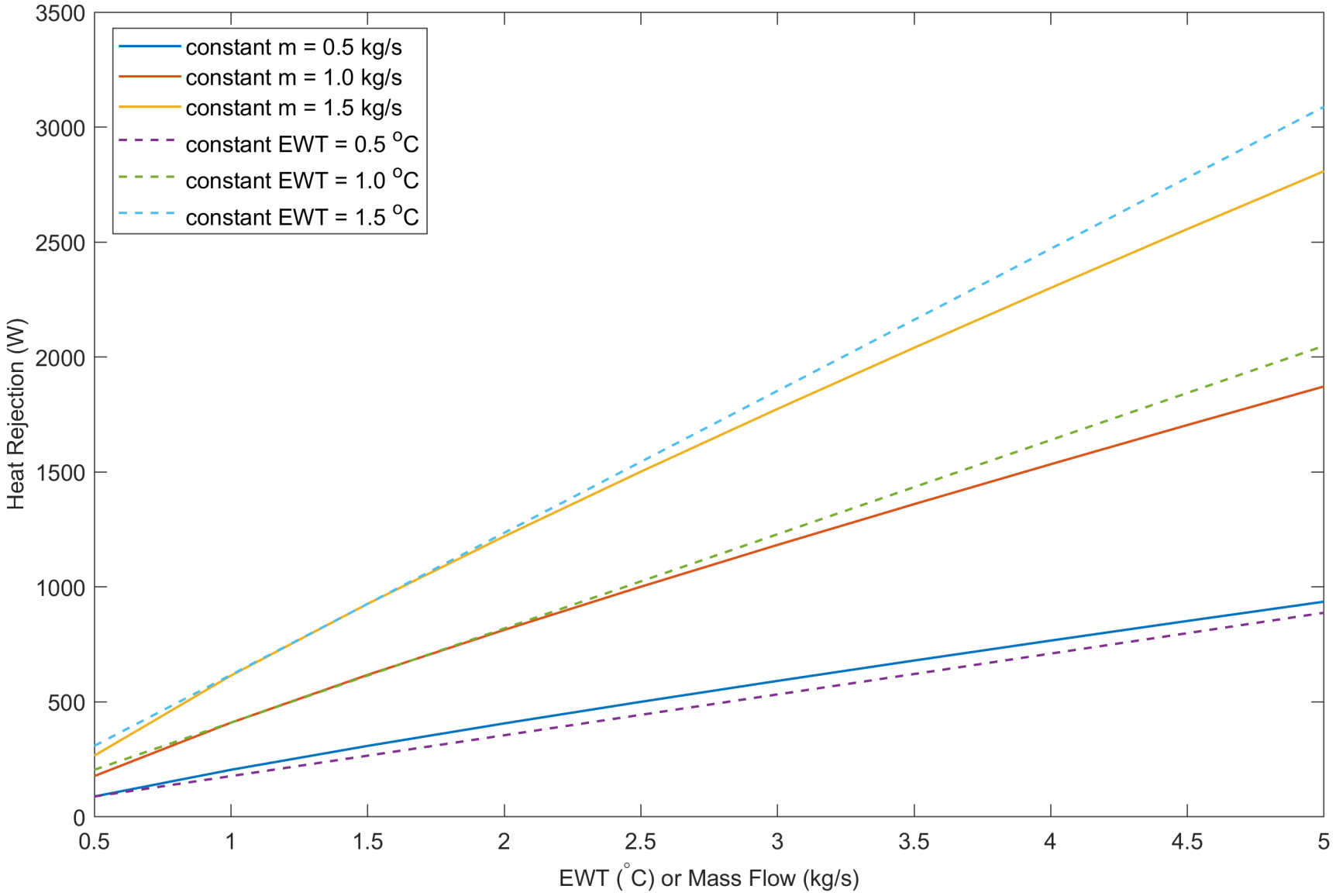

Figure 6-7: Impact of controlling mass flow and EWT on heat rejection for 0 °C soil temperature

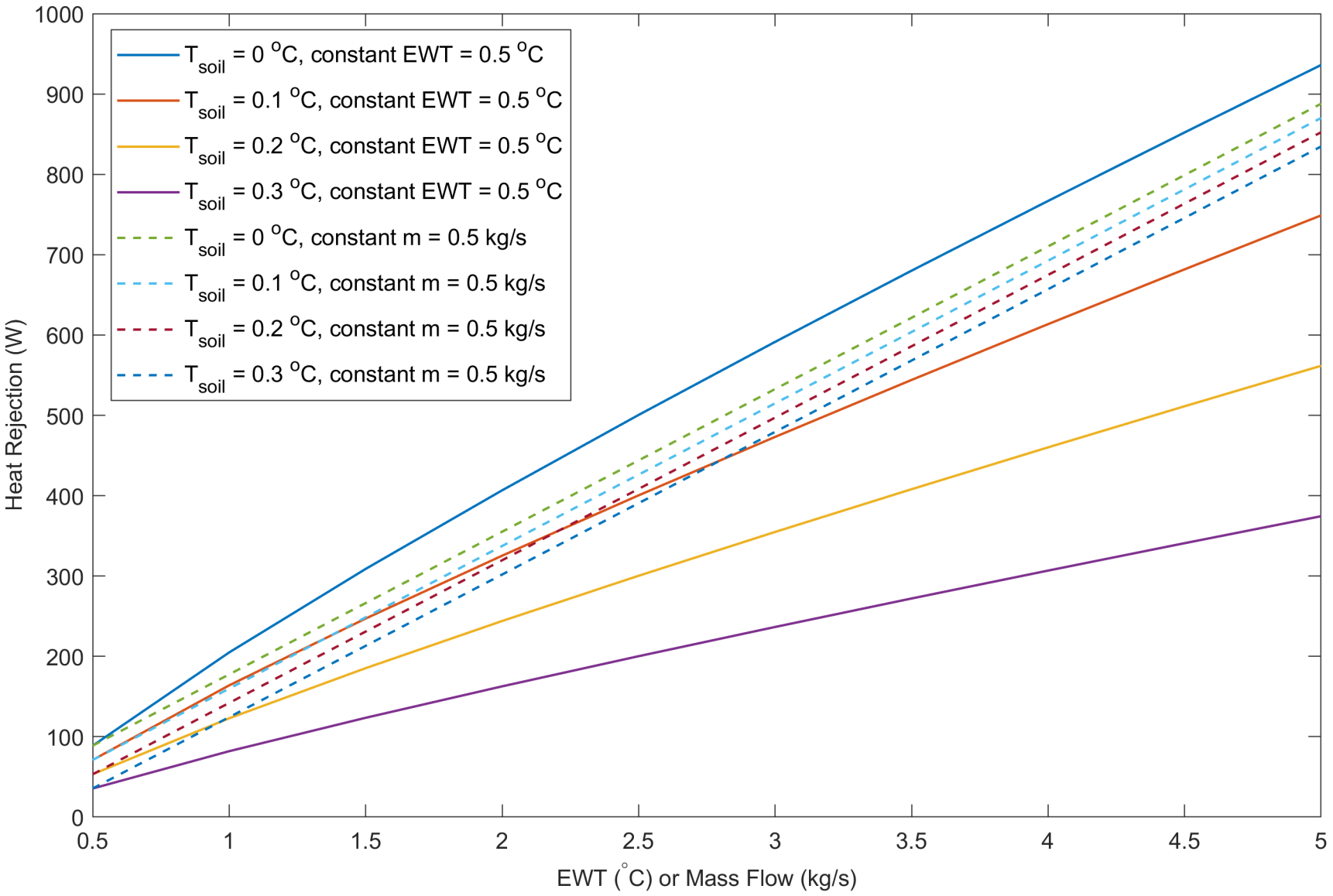

Figure 6-8: Impact of controlling mass flow and EWT on heat rejection for increased soil temperatures

Chapter 7

Conclusion

Thus far, this study has shown that the proposed ground storage cooling system is a feasible option for meeting the latent cooling loads of an office building in the VolpeMIT development. Using the preliminary sizing of Chapter 3, the analysis in Chapters 4 and 5 showed that HX units could successfully charge the soil block over the winter period. The summer modeling in Chapter 6 showed that the system was generally successful in providing sufficiently cold water for dehumidification although the system sizing may need a modest increase to consistently meet the peak load period. Staging the pipes during the summer operation so that they are not all used simultaneously could also potentially resolve the peak load issue without any further changes to the system size.

7.1 System Performance

The energy use of the system is primarily driven by the combined pumping requirements of the soil block piping components and the cooling source heat exchangers. The heat exchangers used for dehumidification would be included in the DOAS regardless of the source of chilled water used. Therefore, the design of these heat exchangers and their subsequent energy use are not included in the calculation of the energy use of the proposed cooling system.

7.1.1 Soil Block Pump Energy

The soil block pump energy estimate is based on the pressure drop due to friction in the 80 pipes and the pressure drop due to the fittings at the end of these pipes. The previous estimate of the pump energy associated with the soil block in Chapter 3 used water flows that were much lower than the actual water flows in the winter and summer modeling. The estimate is corrected by recalculating with the water flow rates used in the two operating modes. It should be noted that the combined soil block pressure drop does not include the pressure drop due to the header piping or the piping that connects it to the other components in the system. Those pipes have not been sized and could be designed to minimize their impact on the overall pipe pressure drop, so they are omitted from the calculation.

During winter charging, $\dot{m}_w$ is 0.5 kg/s and the equipment operates for 2077 hours.

$$u_w = 0.02\,\mathrm{m/s} \tag{7.1}$$

$$\mathrm{Re}_D = 2496 \tag{7.2}$$

$$f = 0.05 \tag{7.3}$$

$$L = 80 \cdot 40\,\mathrm{m} \tag{7.4}$$

$$\Sigma K = 268.8 \tag{7.5}$$

$$\Delta P = \frac{1}{2}\rho u^2\Big(\frac{fL}{D_p} + \Sigma K\Big) = 287\,\mathrm{Pa} \tag{7.6}$$

$$w = 80\frac{\dot{m}_w}{\rho_w}\Delta P = 11\,\mathrm{W} \tag{7.7}$$

$$W = w \cdot 2077\,\mathrm{h} \cdot 3600\,\mathrm{s/h} = 86\,\mathrm{MJ} \tag{7.8}$$

During summer discharging, $\dot{m}_w$ is 1 kg/s and the equipment operates for 1136 hours.

$$u_w = 0.04\,\mathrm{m/s} \tag{7.9}$$

$$\mathrm{Re}_D = 4993 \tag{7.10}$$

$$f = 0.04 \tag{7.11}$$

$$\Delta P = \frac{1}{2}\rho u^2\Big(\frac{fL}{D_p} + \Sigma K\Big) = 967\,\mathrm{Pa} \tag{7.12}$$

$$w = 80\frac{\dot{m}_w}{\rho_w}\Delta P = 77\,\mathrm{W} \tag{7.13}$$

$$W = q \cdot 1136\,\mathrm{h} \cdot 3600\,\mathrm{s/h} = 316\,\mathrm{MJ} \tag{7.14}$$

7.1.2 Combined System Energy Use

As listed in Table 5.2, the cooling source heat exchangers have an overall demand of 568 W and an energy use of 4.25 MJ. The combined fan and pumping demand and energy use of the HX units and the soil block pump is summarized in Table 7.1. The demand has been separated into winter and summer values because the heat exchangers only operate during winter.

Table 7.1: Peak demand and combined energy use of the proposed cooling system

Peak winter demand	579 W
Peak summer demand	77 W
Combined energy consumption	4.65 GJ

Based on this combined system energy consumption, the system Coefficient of Performance (COP) is calculated as

$$\begin{aligned}\mathrm{COP} &= \frac{\text{Annual Building Latent Load}}{\text{Proposed System Energy Use}} \\ &= \frac{332\,\mathrm{GJ}}{4.65\,\mathrm{GJ}} \\ &= 71\ .\end{aligned} \tag{7.15}$$

7.2 Performance Comparison

Table 7.2: Coefficient of Performance (COP) values for comparable systems

System	COP
Proposed ground storage	71
ASHRAE air-cooled screw chiller	
minimum rated COP	2.96
average working hour COP with part-load adjustment	4.11
Chen (2019) systems	
water-cooled chiller	3.33
water-cooled chiller with sensible heat recovery	3.27
water-cooled chiller with enthalpy heat recovery	3.50
desiccant cooling	6.01
membrane cooling	6.29
membrane cooling with membrane	6.05
Yang et al. (2013) system	
vertical borehole ground storage	7.90 to 13.32

Estimating the energy use of a conventional air-cooled screw chiller for meeting the building latent cooling loads provides a comparison for the performance of the proposed system. An air-cooled chiller is used instead of a water-cooled chiller to avoid the added complexity of the cooling tower performance. ASHRAE 90.1-2019 gives the minimum performance for an air-cooled chiller as 10.1 EER (2.96 COP) (ASHRAE, 2019). The chiller is sized as the maximum building latent cooling load divided by this minimum COP, so no oversizing is included. If the air-cooled chiller COP is assumed constant over all hourly latent loads, q, then the hourly chiller energy demand, q_{AC} and energy consumption, Q_{AC} is

$$q_{AC} = \frac{q}{COP} \tag{7.16}$$

$$Q_{AC} = q_{AC} \cdot 3600\,\mathrm{s/h} \tag{7.17}$$

The average hourly chiller demand, dividing over the number of hours with a latent load, is 34.4 kW and the total chiller energy use is 112 GJ.

In reality, chillers do not operate at one constant efficiency for all loads. Applying a

chiller cooling capacity adjustment curve (Goel et al., 2017) to reflect the impact of this variation improved the overall chiller efficiency. The resultant average hourly chiller demand is 24.8 kW and the total chiller energy use is 80.8 GJ. The average COP with the part-load curve included is 4.11.

Several of the other comparable systems described in Section 1.4 were modeled by Chen (2019) to meet the latent cooling loads of an energy-efficient office building in Boston. The building type served and location are the same, so the COP values calculated in his thesis, listed in 7.2, are useful comparisons for the proposed system. The water-cooled chiller systems rely on the vapor-compression cycle to produce sufficiently cold water for dehumidification. The limitations of that method is evident in the relatively low COP values of those systems.

The desiccant and membrane systems draw the water vapor out of the air without condensing. Thus, they are not hindered by any vapor-compression cycle limits and achieve COP values that are almost double those of the chiller systems. Nonetheless, the proposed system vastly outperforms even these next-generation cooling systems, showing that dehumidifying by drawing the moisture out of the humid air, rather than condensing the moisture onto a cold surface is not always more efficient.

The vertical borehole ground storage system developed by Yang et al. (2013) was used to meet the total cooling loads of a test room in Harbin, China. As the location and loads are quite different, the performance ratings are not an exact comparison. However, the high COP values achieved in that study, relative to more conventional systems, support the high performance estimated for the proposed system.

In general, these results show that using cold water for dehumidification is not inherently inefficient. Instead, it is the method of producing the cold water needed that drives the overall system effectiveness. In the case of the conventional water and air-cooled chillers, the overall system COP values are low due to the limitations of the vapor-compression cycle. The vertical borehole ground storage system and the proposed system take advantage of the local weather conditions to produce cold water in winter at a relatively low energy cost, resulting in much higher COP values.

7.3 Functionality in Future Climate

As the climate warms, the need for cooling is expected to grow such that a system sized for current weather may be unable to satisfy future loads. The Climate Change World Weather File Generator tool (CCWWG) created by the University of Southampton (Jentsch et al., 2013) was used to transform the current Boston weather file into its 2050's and 2080's equivalents. Figure 7-1 shows the humidity ratios of the morphed weather file along with the current weather data. It is clear that the peak loads and the number of load hours will increase significantly with climate change.

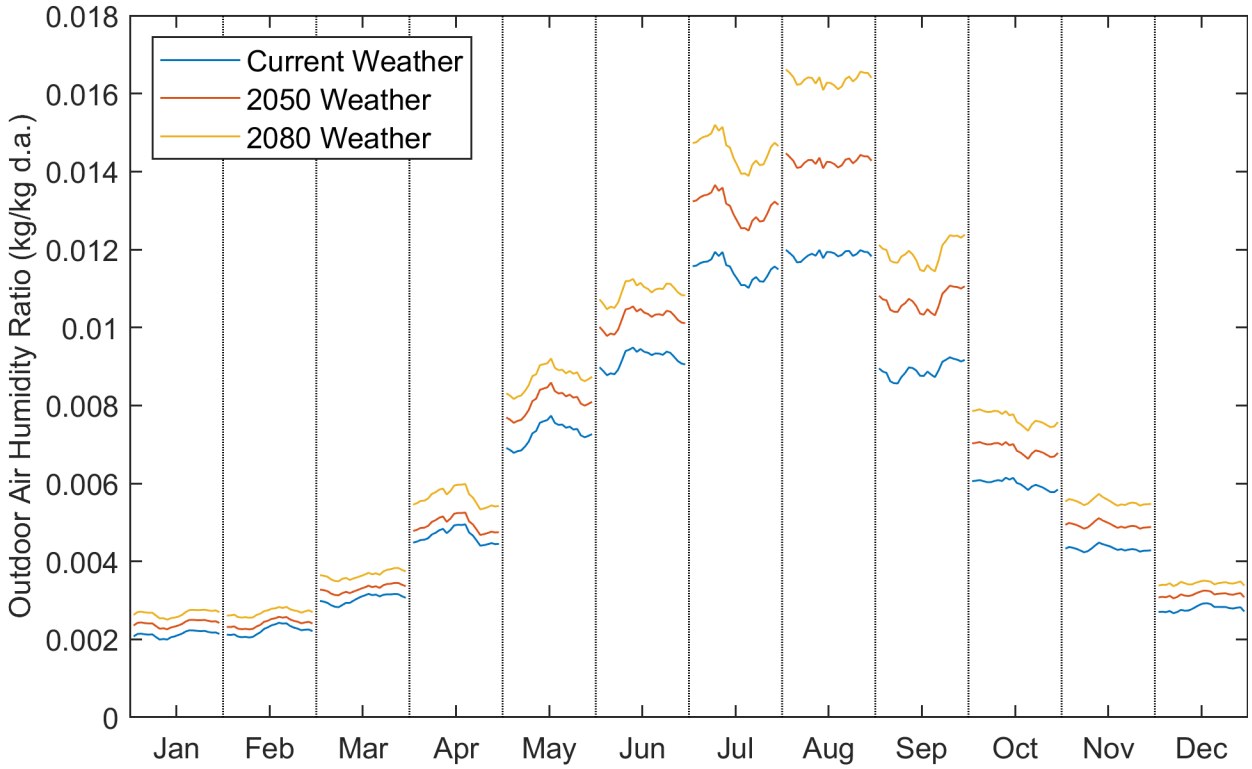

Figure 7-1: Hourly average humidity ratios for current, 2050, and 2080 weather data

The procedure described in Section 2.2 was used with this future weather data to calculate the hourly loads. The results are summarized in Table 7.3 and the daily maximum cooling load values are plotted in Figure 7-2. A soil block sized for the current loads will store sufficient cooling for about half the loads in 2080, so further work is needed to improve the system resilience.

The general warming also has implications for the feasibility of the winter charging be-

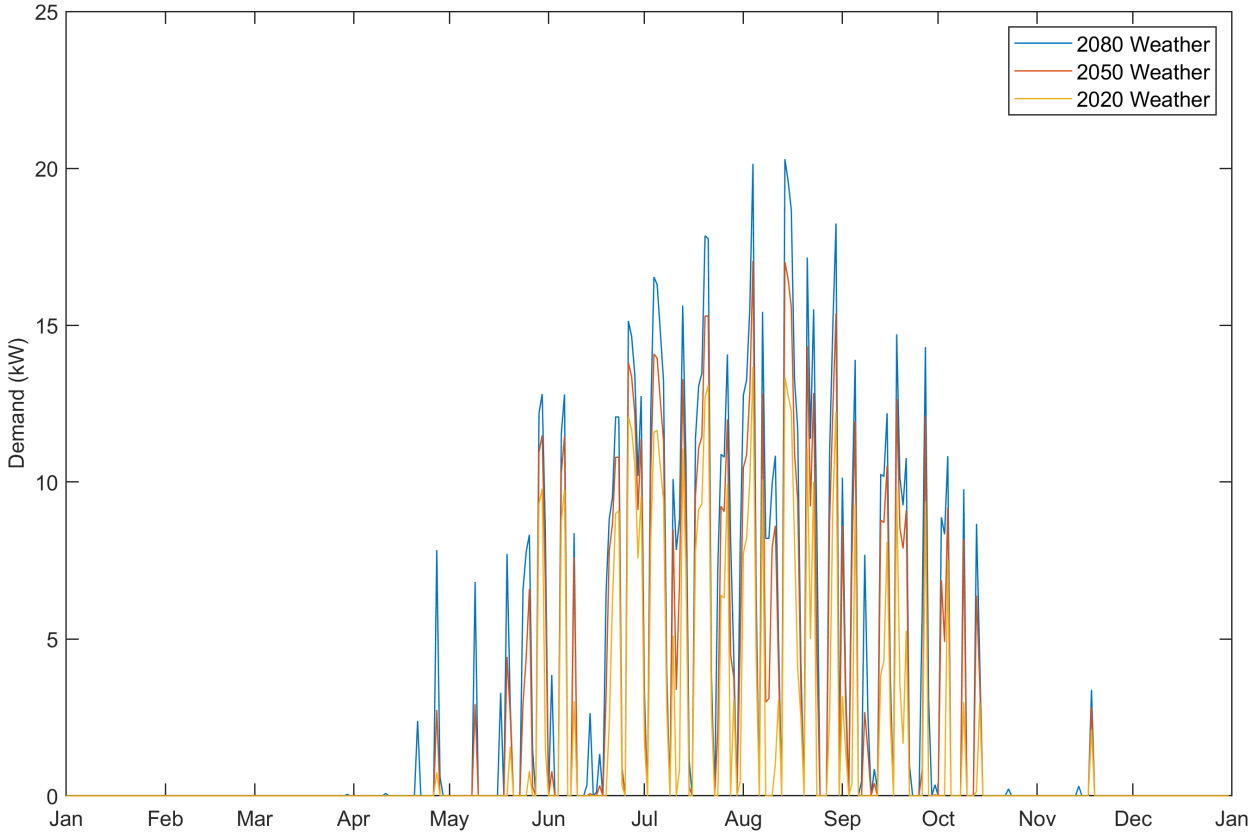

Figure 7-2: Boston office weekly maximum loads for current, 2050, and 2080 weather data

cause there are fewer cold hours available, as shown in Table 7.4. If the soil block volume is kept at its current size, $H_s = 8\,\text{m}$, the 11 HX units will no longer be sufficient to fully charge the block by 2050. In 2050, the number of units would have to increase to 17, although they would run for 1909 hours, which is less than the current 2077 hours. In 2080, there would have to be 28 units, which would run for 1570 hours. If the soil block volume is increased to match the increased loads of the future weather files, the number of units needed for charging would increase even further.

The increased loads calculated for the future weather files suggest that further work is needed to improve the resilience of the proposed system design. Nonetheless, its high performance in comparison to conventional systems make it worth considering regardless. After all, the development and implementation of highly efficient systems is intended to decrease emissions and slow the rate of climate change, such that the future weather may not be as drastically different as currently predicted.

Table 7.3: Summary of building latent cooling loads for current and future weather data

	Current Weather	2050 Weather	2080 Weather
Number of Load Hours	906	1268	1426
Maximum Demand (kW)	343	426	507
Average Demand (kW)	102	117	137
Maximum Consumption (MJ)	1230	1534	1826
Average Consumption (MJ)	366	420	494
Total Consumption (GJ)	332	533	705
Soil Block Height Required (m)	8	13	17

Table 7.4: Subzero outside air temperature counts for current and future weather data

	Current Weather	2050 Weather	2080 Weather
Number of hours with subzero temperature	1252	841	561
Average subzero outside air temperature (°C)	-4.80	-4.09	-3.24

7.4 Future Work

This thesis has shown that the proposed system is a feasible cooling system for the VolpeMIT development and shows potential for significant energy savings in comparison to conventional cooling systems. These promising results indicate that the system is worth further investigation.

The system sizing offers many opportunities for further study. To start, it would be beneficial to conduct a detailed soil study for the site to obtain accurate values for its thermophysical properties, which would improve the system sizing and modeling.

The summer modeling results indicate that increasing the soil block size would help with meeting the peak loads, but at the detriment of the excavation and installation costs. Strategies for meeting these peak loads without increasing the number of pipes should be explored. One possible strategy is using the pipes in the soil block individually, rather than simultaneously, to keep some cold soil in reserve for sudden peaks in cooling loads. Another possible strategy is reducing the pipe diameters and pipe spacing so that there is more soil

available for storage within the soil block. Reducing the number of pipes in the soil block would decrease the material and installation costs of the system.

As mentioned in Chapter 2, the latent cooling loads were calculated from the more stringent thermal comfort limits of the Graphical Comfort Zone Method, resulting in a system that is likely oversized. For a conservative feasibility study, this oversizing was acceptable. However, further work should size the proposed system using a more accurate calculation of the latent cooling loads, based on the Predicted Mean Vote method. It would also be informative to use the PMV thermal comfort method to calculate the latent cooling loads for the future weather files. If the combination of the harsher weather with the more lenient thermal comfort limit results in a soil block sizing that is reasonable, it might be worthwhile to size the system to provide resilience in future.

In this study, the soil block and the heat exchangers are modeled as separate components during the winter charging. The accuracy of the winter charging model would be improved by combining the two components into a single model that simulates the interaction between the outside weather, the heat exchangers, and the soil block. In Chapter 6, it was suggested that the soil block could be charged even during the summer operation, since the latent cooling period extends into November, when the weather is getting colder. Although it would increase the complexity of the model, it would be worth exploring the possibility of charging the soil whenever the outside air is cooler than the soil, rather than operating in distinct seasonal charging and discharging modes. This could improve the ability of the system to meet loads when the cooling potential of the soil block is nearly exhausted and might allow for the soil block size to be further reduced.

Lastly, the system operation should be modeled over several successive years, using measured weather data instead of the median weather data represented in the weather files. For example, an extreme cold snap could reduce the winter charging time needed, reducing the overall energy use. Or perhaps the system might not be sufficiently sized to meet the loads during an unusually humid summer. Using the measured weather data would show if the system can perform consistently, even during years with extreme weather conditions.

Bibliography

Alfa Heating Supply (n.d.). Air to water heat exchangers. Accessed May 2020 from https://alfaheating.com/collections/air-to-water-heat-exchangers.

ASHRAE (2016). *ASHRAE Standard 62.1-2016: Ventilation for Acceptable Indoor Air Quality*. Table 6.2.2.1.

ASHRAE (2017a). *2017 ASHRAE Handbook Fundamentals*. ASHRAE, Atlanta, GA.

ASHRAE (2017b). *ANSI/ASHRAE Standard 55-2017: Thermal Environmental Conditions for Human Occupancy*.

ASHRAE (2017c). *Standard 90.1 User's Manual : ANSI/ASHRAE/IES Standard 90.1-2016: Energy Standard for Buildings Except Low-rise Residential Buildings: I-P and SI.*, chapter Table G-H. Office Occupancy. ASHRAE, Atlanta, GA.

ASHRAE (2019). *ASHRAE Standard 90.1-2019: Energy Standard for Buildings Except Low-rise Residential Buildings*. Table 6.8.1-3.

Bott, C., Dressel, I., and Bayer, P. (2019). State-of-technology review of water-based closed seasonal thermal energy storage systems. *Renewable and Sustainable Energy Reviews*, 113. https://doi.org/10.1016/j.rser.2019.06.048.

Cambridge (2017). Ordinance number 1398. Uploaded to VolpeMIT website February 2020. https://volpe.mit.edu/wp-content/uploads/2020/02/Volpe-Zoning-Text-Feb-2020.pdf.

Chen, T. (2019). *Next-Generation Dedicated Outdoor Air Cooling Systems for Low-Energy Buildings*. PhD thesis, Massachusetts Institute of Technology, Department of Mechanical Engineering.

EIA (2016). 2012 commercial buildings energy consumption survey. Table E1, EIA, Washington, D.C., USA.

EIA (2018). 2015 residential energy consumption survey. Table CE3.1, EIA, Washington, D.C., USA.

EIA (2020). U.S. energy consumption by source and sector, 2019. Annual energy review, EIA, Washington, D.C., USA.

Engineering ToolBox (2003). Specific heat of some common substances.

Engineering ToolBox (2010). Dirt and mud - densities.

Goel, S., Rosenberg, M. I., and Eley, C. (2017). ANSI/ASHRAE/IES standard 90.1-2016 performance rating method reference manual. Technical Report PNNL-26917, Pacific Northwest National Laboratory, Richmond, WA.

Goetzler, W., Guernsey, M., Young, J., Fujrman, J., and Abdelaziz, A. (2016). The future of air conditioning for buildings. report, US Department of Energy.

Google (n.d.). Google map of Cambridge area around VolpeMIT site. Retrieved July 8, 2020 from https://goo.gl/maps/iy7VntswqqMFikPR7.

Hoyt, T., Schiavon, S., Tartarini, F., Cheung, T., Steinfeld, K., Piccioli, A., and Moon, D. (2019). CBE thermal comfort tool. Center for the Built Environment, University of California Berkeley.

Incropera, F. P. and DeWitt, D. P. (2002). *Fundamentals of Heat and Mass Transfer*. Wiley.

IPCC (2014). Climate change 2014: Synthesis report. contribution of working groups I, II and III to the fifth assessment report of the intergovernmental panel on climate change. [Core Writing Team, R.K. Pachauri and L.A. Meyer (eds.)], IPCC, Geneva, Switzerland.

Jentsch, M. F., James, P. A., Bourikas, L., and Bahaj, A. S. (2013). Transforming existing weather data for worldwide locations to enable energy and building performance simulation under future climates. *Renewable Energy*, (55):514–524.

Lindsay, B. B. and Andrepont, J. S. (2019). Evolution of thermal energy storage for cooling applications. *ASHRAE Journal*, pages 42–59.

MATLAB (2018). *version 9.4.0 (R2018a)*. The MathWorks Inc., Natick, Massachusetts.

National Renewable Energy Laboratory (n.d.). Boston-Logan Intl AP 725090 (TMY3). Retrieved September 30, 2019 from https://energyplus.net/weather.

Roudsari, M. S. and Pak, M. (2013). Ladybug: a parametric environmental plugin for grasshopper to help designers create an environmentally-conscious design. In *Proceedings of the 13th International IBPSA Conference*, Lyon, France.

Sokolov, A., Gao, X., Paltsev, S., Monier, E., Chen, H., Kicklighter, D., Prinn, R., Reilly, J., and Schlosser, A. (2017). Probabilistic projections of the future climate for the world and the continental USA. *Joint Program Report Series* ***Report 320***.

Yang, T., Zhang, X., Zhou, B., and Zheng, M. (2013). Simulation and experimental validation of soil cool storage with seasonal natural energy. *Energy and Buildings*, (63):98–107. https://doi.org/10.1016/j.enbuild.2013.03.019.

Appendix A

Hourly Latent Load Calculation

```
% WEATHER
% hourly weather file with humidity ratios calculated
weather = readtable(`BostonOAHR.csv');
OAHR = weather.OAHR;    % hourly outdoor air humidity ratios (
   kg/kg d.a.)
% PHYSICAL PARAMETERS
AirDensity = 1.23;       % dry air density (kg/m^3)
h_fg = 2500e3;  % latent heat of vaporisation for approximately
    0C water (J/kg)
% BUILDING PARAMETERS
Area = 40*44;   % floor area (m^2)
numFloors = 25; % number of floors in building
OccRate = 0.1;  % occupancy rate (people/m^2)
VentRate = (8.5/1000)*AirDensity;  % ASHRAE combined
   ventilation rate for office (kg/s*person)
WheelEff = 0.75;    % Enthalpy wheel effectiveness
% LATENT LOAD DUE TO OCCUPANTS
OccLoad = 45;   % ASHRAE Fundamentals 2017 Ch18 Table 1, seated
    light work (W per person)
```

```
OccLoad = OccLoad/h_fg;          % moisture added by people (kg/
   s*person)
dHR = OccLoad / VentRate;        % moisture added to room air
   due to occupants (kg/kg)
% THERMAL COMFORT LIMIT
HRlim = 0.012 - dHR;  % maximum allowable OAHR for comfort (kg/
   kg d.a)

% CREATE SCHEDULES
% HVAC
% Weekday HVAC ON/OFF Schedule
HVAC.WDSch = [zeros([6,1]);ones([16,1]);zeros([2,1])]';
% Saturday HVAC ON/OFF Schedule
HVAC.SatSch = [zeros([6,1]);ones([12,1]);zeros([6,1])]';
% Sunday HVAC ON/OFF Schedule
HVAC.SunSch = zeros([1,24]);
% Weekly HVAC ON/OFF Schedule
HVAC.WkSch = [HVAC.SunSch, repmat(HVAC.WDSch, 1,5), HVAC.SatSch
   ]';
% Annual HVAC ON/OFF Schedule (52 weeks + 1 Sunday)
HVACSch = [repmat(HVAC.WkSch, 52,1); (HVAC.SunSch)'];

% Occupancy
% Weekday OCC ON/OFF Schedule
OCC.WDSch = [zeros([6,1]); 0.1; 0.2; 0.95*ones([4,1]); 0.5;
   0.95*ones([4,1]); 0.3; ...
    0.1*ones([4,1]); 0.05*ones([2,1])]';
% Saturday OCC ON/OFF Schedule
OCC.SatSch = [zeros([6,1]); 0.1*ones([2,1]); 0.3*ones([4,1]);
   0.1*ones([5,1]); ...
```

```
    0.05*ones([2,1]);zeros([5,1])]';
% Sunday OCC ON/OFF Schedule
OCC.SunSch = [zeros([6,1]); 0.05*ones([12,1]); zeros([6,1])]';
% Weekly OCC ON/OFF Schedule
OCC.WkSch = [OCC.SunSch, repmat(OCC.WDSch, 1,5), OCC.SatSch]';
% Annual OCC ON/OFF Schedule (52 weeks + 1 Sunday)
OCCSch = [repmat(OCC.WkSch, 52,1); (OCC.SunSch)'];

% CALCULATE LATENT LOADS
% if OAHR < room HR, ERV bypassed (SAHR = OAHR)
% if OAHR > room HR, ERV used to reduce SAHR (SAHR != OAHR)
SAHR = OAHR - WheelEff*(max(OAHR, 0.012) - 0.012);      %
   supply air humidity ratio (kg/kg d.a.)
% number of people * delta HR * air flow * h_fg
Load = (OccRate*Area*OCCSch).*(SAHR - HRlim).*VentRate*h_fg;
       % latent cooling demand (W)
% limit load to hours when HVAC equipment is on
Load = Load.* HVACSch;
% remove any negative loads (no dehumidification needed)
Load(Load<0) = 0;

fDem = Load;            % hourly floor demand (W)
bDem = numFloors*Load;  % hourly building demand (W)
fCon = 60*60*Load;      % hourly floor consumption (J)
bCon = numFloors*fCon;  % hourly building consumption (J)
```

Appendix B

Winter Charging Simulation

```
% SETUP
tlist = 0:200:(60*60*24*30*3);  % 3 month charging period with
   200s timestep
% Load PDE model with geometry, mesh, and soil material
   properties defined.
load model.mat
% set initial temperature condition
thermalIC(model, 10);   % degC

% array to store pipe temeperatures for all slices at each
   timestep
pipeTemps = zeros([9, length(tlist)], 'single');

% SLICE SIMULATION
% Slice 1
% Pipe BC: constant temperature of 0 degC
thermalBC(model, 'Edge', [5 6 7 8], 'Temperature', 0);
result = solve(model, tlist);
sliceTemps(:,:,1) = single(result.Temperature);
```

```
% Slices 2 to 9
for i = 2:9   % iterate over remaining slices
  % calculate temperatures at each timestep for pipe BC
  PT = getWaterTemp(model, 0.3625*200, result, pipeTemps(i-1,
     :));
  pipeTemps(i, :) = PT;
  % apply pipe temperatures to transient slice model as BC
     function
  TFunc = @(region, state) BCFunc(region, state, PT);
  thermalBC(model, 'Edge', [5 6 7 8], 'Temperature', TFunc);
  result = solve(model, tlist);
  sliceTemps(:,:,i) = single(result.Temperature);
end

% BC FUNCTION
function f = BCFunc(region, state, BCtemp)
if isnan(state.time)
    f = nan(size(region.x));
else
    f = BCtemp(floor(state.time/200)+1) * ones(1, length(region
       .x));
end
end
```

Appendix C

Summer Charging Simulation

```
% SETUP
% Load PDE model with geometry, mesh, and soil material
   properties defined.
load model.mat
% Load daily Building latent cooling demand loads averaged over
    16 hours
load('BosOfcLatentLoad.mat', 'qAvgD')
[dRange(1), dRange(2)] = bounds(find(qAvgD>=0));  % first and
   last day with load
% Variables
numPipes = 80;  % number of pipes used to meet the load
qAvgD = (1/numPipes)*qAvgD;     % distribute load over all
   pipes
massFlow = 1;   % kg/s, initial mass flow rate
% Create files for storing results
for i = 1:9
    filenameST(i) = join(['Summer\', datestr(date, 'yyyymmdd'),
        ...
        '_soilTemps', num2str(i), '.csv']);
```

```
    writematrix([], filenameST(i));
end
filenameET = join(['Summer\', datestr(date, 'yyyymmdd'), ...
    '_entTemps.csv']);
writematrix([], filenameET);
filenameLT = join(['Summer\', datestr(date, 'yyyymmdd'), ...
    '_lvgTemps.csv']);
writematrix([], filenameLT);

% RUN SUMMER
initCond = {0};  % degC, initial condition of 0 degC for soil
for d = dRange(1):dRange(2)
    if d == dRange(1)     % first day of cooling
        entTemp = getEntWaterTemp(zeros([length(model.Mesh.
            Nodes), ...
                    1, 9]), 1.15*qAvgD(d), 0.15);
    elseif qAvgD(d) > 0   % cooling required and not first day
        % use the lower of previous entTemp and entTemp
            calculated for
        % latest load & soil condition
        entTemp = min(getEntWaterTemp(soilTD(:,end,:), 1.15*
            qAvgD(d), ...
                    max(soilTD(:,end,:), [], 'all')), entTemp);
    end
    % run model
    [soilTD, entTempD, lvgTempD, initCond] = RunSummerDay(...
        model, initCond, entTemp, qAvgD(d));
    entTemp = max(entTempD(480), entTemp);
    % append results into results files
    for i = 1:9
```

```
        dlmwrite(filenameST(i), transpose(soilTD(:, 1:30:end, i
            )), ...
              '-append', 'delimiter', ',');
    end
    dlmwrite(filenameET, entTempD(1:30:end), '-append', '
       delimiter', ',');
    dlmwrite(filenameLT, lvgTempD(1:30:end), '-append', '
       delimiter', ',');
    clearvars entTempD lvgTempD
end

%% Heat Rejection
Tin = readmatrix(filenameET);
Tout = readmatrix(filenameLT);
qR = single(massFlow*4200*(Tin-Tout));
Q = trapz(60*60,qR(~isnan(qR))); % total heat rejected in run
   period
```

C.1 Entering Water Temperature Subfunction

```
function T_in = getEntWaterTemp(soilTemps, Qlimit, Tguess)
% estimate the entering water temperature needed to meet the
   latent load
% INPUTS:
%   soilTemps: temperature of all soil slices at that instant
%   Qlimit: latent cooling load to be met
%   Tguess: initial guess for suitable entering water
   temperature
% OUTPUTS:
%   T_in: entering water temperature that satisfies load
```

```
% water energy balance:
%   massFlow * c_p * (dT/dx) = -h * pi * D * (T - Tsoil(x))
% water temperature function:
%   T(x) = c*theta + Tsoil(x)

% theta calculated from old functions and result copied to save
    time.
% Correct for D = 0.17m & massFlow = 1kg/s
theta = 0.895904541015625; % (T_w(x2) - T_wall)/(T_w(x1) -
   T_wall)

% array of identifiers for nodes that are on the pipe boundary
   in the mesh
pipenodes = single([5 509 23 743 6 619 51 598 7 538 50 610 8
   450 22 693]);
% average temperature of soil at the pipe boundary
Tsoil = single(reshape(mean(soilTemps(pipenodes, :, :)), [1,
   9]));

q = 0;
q_prev = 0;
Tguess_prev = Tguess;
while q < Qlimit
Tout = Tguess;
% calculate the leaving water temp
for i = 1:length(Tsoil)
    % assuming soil temp is constant over slice
    Tout = theta*(Tout - Tsoil(i)) + Tsoil(i);
end
q = 1*4200*(Tguess - Tout);
```

```
if q < Qlimit
    Tguess_prev = Tguess;
    Tguess = 1.1*Tguess;
    q_prev = q;
end
end

% interpolate between previous value (when q < Qlimit) and
   current
% value (q >= Qlimit). Returns Tcurr if q = Qlimit.
T_in = interp1([q,q_prev], [Tguess,Tguess_prev], Qlimit);
end
```

C.2 Run Summer Day Subfunction

```
function [soilTD, entTempArr, lvgTempArr, initCond] =
   RunSummerDay(...
    model, initCond, entTemp, q)
% returns results for model of one day
% INPUTS:
%   model: PDE model with geometry, mesh, and material
   properties defined
%   initCond: initial conditions for soil temperatures at mesh
   nodes
%   entTemp: entering water temperature for slice 1
%   q: daily latent load to be met
% OUTPUTS:
%   soilTD: soil temperatures for all slices over day
%   entTempArr: entering water temperatures used
%   lvgTempArr: leaving water temperatures achieved
```

```
%   initCond: final soil conditions (to be used as initial
   condition of following day)

if q <= 0 % no latent load to be met
    tlist = 0:200:60*60*24; % simulate entire day at once
    % soil temperatures over adiabatic day
    [soilTD, initCond] = NoLoad(model, tlist, initCond);
    % store entering water temperatures as nan
    entTempArr(length(tlist)) = nan;
    % store leaving water temperatures as nan
    lvgTempArr(length(tlist)) = nan;
    return
else
    soilTD = zeros([length(model.Mesh.Nodes), 721, 9], 'single'
       );
    lvgTempArr = zeros([1,721], 'single');
    entTempArr = zeros([1,721], 'single');
    tlist = 0:200:60*60*8;  % simulate 8-hour period
    n = 1;
    notmet = 1; % count times load not met at all
    while n < 481   % meet load while equipment on
        [soilT, waterT, initCond] = HasLoad(model, tlist,
           initCond, ...
                                           entTemp, q, n);
        if ~isempty(soilT)
            soilTD(:, n:(n-1)+length(waterT), :) = soilT;
            lvgTempArr(n:(n-1)+length(waterT)) = waterT;
            entTempArr(n:(n-1)+length(waterT)) = entTemp;
            n = n + length(waterT);
            notmet = 1; % reset counter
```

```
            if length(waterT) < length(tlist) % load met
               partially
                % recalculate entTemp
                entTemp = getEntWaterTemp(soilT(:,end,:), 1.15*
                   q, entTemp);
            end
        % load was not met at all
        elseif isnumeric(initCond{1,1})
            notmet = notmet + 1;
            entTemp = getEntWaterTemp(zeros([length(model.Mesh.
               Nodes), ...
                    1, 9]), (1.2^notmet)*q, entTemp);
        else
            notmet = notmet + 1;
            entTemp = getEntWaterTemp(IC2ST(initCond, ...
                    length(model.Mesh.Nodes)), (1.2^notmet)*q,
                       ...
                    entTemp);
        end
    end
    tlist = 0:120:60*60*8;
    % equipment off adiabatic run
    [soilT, initCond] = NoLoad(model, tlist, initCond);
    soilTD(:, n:end, :) = soilT;
    entTempArr(n:end) = nan;
    lvgTempArr(n:end) = nan;
end
end

function [res, ICs] = NoLoad(model, tlist, ICs)
```

```
% no load to be met, so run model with adiabatic pipe boundary
   condition
res = zeros([length(model.Mesh.Nodes), length(tlist), 9], '
   single');
thermalBC(model, 'Edge', [5 6 7 8], 'HeatFlux', 0);
for i = 1:9
    if isnumeric(ICs)   % IC of 0
        thermalIC(model, ICs);
    else
        thermalIC(model, ICs{i,1}, ICs{i,2});
    end
    result = solve(model, tlist);
    res(:,:,i) = single(result.Temperature);
    [ICs{i,1}, ICs{i,2}] = getThermalResult(result, tlist(end))
       ;
end
end

function [res, LT, ICs] = HasLoad(model, tlist, ICs, entTemp, q
   , n)
% meeting load q, so run model with convection pipe boundary
   condition
res = zeros([length(model.Mesh.Nodes), length(tlist), 9], '
   single');
% heat transfer coefficient and theta calculated from old
   functions
% and result copied to save time.
% Correct for D = 0.17m & massFlow = 1kg/s
h = 172.8871459960938;  % W/m^2 K
theta = 0.895904541015625; % (T_w(x2) - T_wall)/(T_w(x1) -
```

```
   T_wall)

% Slice 1
if isnumeric(ICs{1,1})   % IC of 0
    thermalIC(model, ICs{1,1});
else
    thermalIC(model, ICs{1,1}, ICs{1,2});
end
thermalBC(model, 'Edge', [5 6 7 8], 'ConvectionCoefficient', h,
    ...
    'AmbientTemperature', entTemp);
result = solve(model, tlist);
res(:,:,1) = single(result.Temperature);

% Slices 2 to 9
AmbT = entTemp;
for i = 2:9
    % node 8 = node on pipe edge
    if isnumeric(ICs{1,1})   % IC of 0
        thermalIC(model, ICs{1,1});
    else
        thermalIC(model, ICs{i,1}, ICs{i,2});
    end
    % leaving water temp
    LT = theta*(AmbT - res(8,:,i-1)) + res(8,:,i-1);
    AmbT = double(mean(LT));
    thermalBC(model, 'Edge', [5 6 7 8], 'ConvectionCoefficient'
       , h, ...
        'AmbientTemperature', AmbT);
    result = [result; solve(model, tlist)];
```

```
    res(:,:,i) = single(result(i).Temperature);
end
reject = single(1 * 4200 * (entTemp - LT)); % W
% find when load last met or when equipment last on
lastMet = single( min(find(reject >= 0.85*q , 1, 'last'), 481-n
   ) );
if ~isempty(lastMet)
    % truncate to the times load met
    res = res(:, 1:lastMet, :);
    LT = LT(1:lastMet);
    lastMet = min(lastMet, length(tlist)-1);
    for i = 1:9
        % initial condition of each slice is the final
           temperature of that slice
        [ICs{i,1}, ICs{i,2}] = getThermalResult(result(i),
           lastMet*120);
    end
else    % load never met
    res = [];
    LT = [];
end
end

function [resultIndex, timeIndex] = getThermalResult(
   sliceResults, solutionTime)
% function thermalResult = getThermalResult(sliceResults,
   solutionTime)
% find which thermal result for a slice should be used for the
   initial
% condition of that slice
```

```
for i = 1:length(sliceResults)
    % see if solution time is in list of solution times of the
       result
    temp = find(sliceResults(i).SolutionTimes == solutionTime);
    if (~isempty(temp))
        rI = i;    % which result holds that solution time
        tI = temp;   % index of the solution time within that
           result
    end
end
% return the indices
resultIndex = sliceResults(rI);
timeIndex = tI;
end
function ST = IC2ST(IC, meshSize)
% get soil temperatures from initial conditions
ST = zeros([meshSize, 1, 9], 'single');
for i = 1:9
    result = IC{i,1};
    ST(:,:,i) = result.Temperature(:,IC{i,2});
end
end
```